METHOD FOR THE PREDICTION OF PERFORMANCE OF STOL HIGH LIFT SYSTEMS NEAR $C_{L_{max}}$

PAUL T. BAUER

UNIVERSITY OF DAYTON
RESEARCH INSTITUTE

FOREWORD

This report was prepared by the University of Dayton Research Institute (UDRI) under USAF Contract No. AF33615-70-C-1019. This work was conducted for the V/STOL Technology Division, Air Force Flight Dynamics Laboratory. The Air Force Project engineer was Capt. Forrest Stoddard.

This study was performed from January 1971 to September 1971 by Dr. P. T. Bauer of the University of Dayton.

This technical report has been reviewed and has been approved.

Ernest J. Cross Jr.

ERNEST J. CROSS, JR.
Lt. Col., USAF
Chief, Prototype Division

ABSTRACT

Potential flow and boundary layer methods are identified and developed for the analytic calculation of the performance of lift systems with significant flow separation. Particular emphasis is given to the use of the presented methods in the calculation of the flow field for a single airfoil in demonstration of their capability. A procedure for application to multiple element high lift systems is indicated. Special consideration is given to the representation of turbulent separating boundary layers and an empirical computational procedure has been developed where none had previously existed. The work presented herein provides a thorough basis on which to develop an accurate computer simulation model of high lift systems with significant flow separation.

TABLE OF CONTENTS

LIST OF ILLUSTRATIONS

SECTION I

INTRODUCTION

The objective of this work is to determine, develop and assess methods applicable to the prediction of the performance of high lift systems associated with STOL aircraft under conditions where significant flow separation occurs from the various lifting elements. Presently, no single procedure has been developed for such an application. In order to achieve this objective, attention was limited to the consideration of separation from a simple airfoil with eventual application as a future project as a guiding restriction. Nonetheless, there is presented in this work procedures for the application of the presented methods to the analysis of multiple element high lift systems.

With regard to the study of separated flow from an airfoil, the following specific areas were of particular interest: (1) the pressure distribution on the suction side of the airfoil in the separated wake region, (2) potential flow models of airfoil flow with separation, and (3) boundary layer computation techniques for laminar, transitional, turbulent, and separating flow. Each of these areas have been examined and adequate methods have been identified for performance calculations of airfoils when separation occurs and where stall is caused by the forward movement, from trailing edge, of the location of turbulent separation.

In the following sections of this report, there are presented existing computation schemes appropriate to this research program. In addition, a method for the representation of turbulent separation is presented. Prior to this research effort there did not exist any such method. Moreover, the discussion of the computational representation of separation includes special emphasis on the relationship between actual (experimental) pressure distributions and that computed by potential, separated flow, solutions. It is this relationship that is the key to both a successful boundary layer calculation and improved prediction of pressure distributions.

For the sake of organization and clarity, the remainder of this section discusses the type of airfoil of stall of particular interest to this research effort. Next is presented a section on potential flow solutions with particular emphasis on a technique that has been overlooked in contemporary literature. This technique combines a previously recognized computation scheme for potential flow without separation with a relatively new approach to the potential flow representation of separation. There is then presented a discussion of a potential model for high lift systems with separation.

A section on the relevant boundary layer computation methods follows the section on potential flow solutions. The most appropriate existing methods for the computation of laminar, transitional, and turbulent flows are described, together with the reasons for their selection. There is then presented a comparison of computations, using the selected methods, with experimental data. Finally, a new method, developed under this research program, for the representation of a separating turbulent boundary layer is presented.

A final section presents recommendations for future development.

A. STALL CHARACTERISTICS

Before discussion the work of this research effort, it is instructive to first review the mechanisms which cause an airfoil to stall. Three basic categories of stall have been established (Ref. 1). While the stall of any given airfoil may not be confined to any one of these categories, they are useful in providing broad trends. The three categories are (see Figure 1):

1. stall caused by the continuous forward progress from the trailing edge of a turbulent separating boundary layer,
2. stall caused by the bursting of a "short bubble", and
3. stall caused by the growth of a "long bubble" beyond the trailing edge.

Each type of stall has been associated with airfoil thickness. It should be noted, however, that Reynolds number also is important in controlling the manner in which an airfoil stalls (Ref. 2). For the Reynolds numbers of STOL aircraft, the relationship between stall characteristic and thickness, discussed below, is appropriate.

For moderate to thick ($t/c > 15\%$) airfoil sections turbulent boundary layer separation starts at the trailing edge. As the angle of attack is increased, the location of separation moves forward with stall occurring when this location reaches about the 50% chord station. Further increase in angle of attack moves the location of separation still further forward. The lift curve and pressure distribution at stall are shown as curves 1 in Figure 1.

Moderately thick ($t/c \cong 9\%$) airfoil sections have a short bubble just past the suction peak. This bubble is formed by a laminar separation, transition in the separated flow, and a turbulent reattachment. This bubble extends over a length of the order of 1% of the chord. Increasing the angle of attack beyond that angle at which the bubble formed tends to shorten the length of the bubble. At stall the bubble "bursts", turbulent reattachment does not occur, and the flow is fully separated. Curves 2 in Figure 1 present the

lift curve and a pressure distribution for an angle of attack prior to stall. The constant pressure "step" just past the pressure peak indicates the presence of the bubble.

On thin ($t/c \cong 6\%$) airfoil sections, a bubble also forms at some angle of attack. However, turbulent reattachment does not occur as rapidly as on moderately thick sections. Furthermore, as the angle of attack is increased, the bubble tends to increase in contrast to the shortening of the bubbles described in the previous paragraph. Stall occurs when these long bubbles grow beyond the trailing edge. Curves 3 of Figure 1 are the lift curve and sample pressure distribution for a condition prior to stall.

The research discussed herein is concerned with the stall associated with the separation of the turbulent boundary. Consideration of stall due to the bursting of long and short bubbles is essentially a boundary layer problem and, at present, an insufficient quantitative basis exists for analysis of airfoils where these phenomena are dominant. Moreover, moderate to thick airfoil sections are of interest to the development of STOL aircraft.

B. FLOW CHARACTERISTICS OF AIRFOIL STALL DUE TO TURBULENT BOUNDARY LAYER SEPARATION

In Figure 2, there is presented an exaggerated sketch of the flow about an airfoil at a lift coefficient near $C_{L_{max}}$. On the suction side of the airfoil, a laminar boundary layer begins at stagnation near the leading edge and grows until transition occurs near the suction pressure peak. Following transition, a turbulent boundary layer commenses to grow until separation occurs. Beyond separation, a dead wake region is formed and bounded by the separated free streamline and the airfoil surface. Because the dynamic pressure in the wake is negligibly small, a significant pressure gradient can not be sustained in any direction in the wake. Hence, the pressure along both the airfoil surface and the separated streamline may be taken as constant, to a high degree of approximation, up to the trailing edge. Weak vortices may exist in the wake between the airfoil surface and the free streamline. Any such vortices, which appear to exist for large wakes, produce only very slight variations in the pressure at the airfoil surface. Beyond the trailing edge, the pressure along the separated free streamline ultimately adjusts to the undisturbed free stream static pressure.

On the pressure side (bottom) of the airfoil, boundary layer growths with transition occur in much the same fashion as on the suction side except, of course, that separation does not occur. It

should be noted that, on the bottom side of the trailing edge, the pressure is approximately that of wake pressure on the suction side. This condition represents a sort-of modified Kutta condition.

The above described flow may be modeled with the combination of a potential flow solution with boundary layer solutions. As is evident from the above discussion, potential flow solutions that satisfy the classical Kutta condition are inadequate. Below is presented a solution which is capable of calculating the potential flow about an airfoil with separation.

The necessary boundary layer solutions also require careful attention. Not only is it necessary to predict the location of transition, but, in addition, separation must also be predicted. An extensive discussion of boundary layer computation schemes follows that of potential flow solution. Special emphasis is given to the prediction of separation.

SECTION II

POTENTIAL FLOW SOLUTIONS

The computation of potential (inviscid) flow about an airfoil without separation can be accomplished in several ways. Classically, various complex transformations (Ref. 3) have been used to describe simple airfoil flows without separation. Such techniques are not appropriate to the general application of interest to this research. More recently, with the advent of the digital computer, other methods have been developed which readily permit the calculation of the potential flow of arbitrary multiple segmented high lift systems without separation. The most popular schemes are those presented in References 4, 5, and 6.

The method of Reference 4 uses a system of source-sink flows distributed along the surfaces of the multiple element airfoils with vorticity distributions contained within the elements of the lift system. In contrast, the method of Reference 5 uses a system of vortex sheets to represent the surfaces of a multi-element lift system. The method of Jacob and Riegels (Ref. 6) uses a system of isolated vortices, rather than vortex sheets as in Reference 5, distributed along the multi-element surfaces. Each of these three methods may be and, in some cases have been, extended to three-dimensional wing flow.

Several investigators, starting with Helmholtz, have attempted to describe a separated potential flow (see Reference 7 and references in Reference 8). Those efforts used complex transformations and where confined to such simple geometries as a flat plate at an angle-of-attack. Hurley (Ref. 9) recently has attempted, with the use of a Schwarz-Christoffel transform and assumptions concerning the shape of the separated free streamline, to develop a potential flow solution. His efforts have, at best, produced only qualitative results.

Jacob (Ref. 10) has extended his earlier method (Ref. 6) by adding a source flow along that portion of the surface of the airfoil wetted by the wake. The concept is to represent the blockage effect of the wake by a source flow from the airfoil. It is required that the pressure of the separated streamline be constant up to a point opposite the trailing edge. The magnitude of this pressure is equal to that at the separation point. The local of separation is based on a boundary layer calculation. The method is presently limited to two-dimensional airfoil sections without flaps or slats.

A. ESSENTIAL FEATURES OF JACOB'S METHOD

Jacob computes the separated potential flow about an airfoil with the superposition of four basic flows (see Figure 3): (1) a uniform flow at zero angle of attack with free stream velocity equal to unity and the total circulation equal to zero, (2) a flow similar to that of (1) but with angle of attack equal to ninety degrees, (3) a circulatory flow of magnitude 2π and with free stream velocity equal to zero, and (4) a source flow essentially from the portion of the airfoil surface wetted by the wake (a small segment of this source flow extends over the bottom side of the airfoil at the trailing edge) with the free stream velocity and vorticity equal to zero. It should be noted that the first three solutions could be combined to determine the classical potential flow about an airfoil without separation. However, the desired separated potential flow is not simply the linear addition of the four solutions since the classical Kutta condition is not employed for the separated flow solution.

In order to determine the required solutions the orthogonal coordinates of the discrete vortices are related to a monotonically increasing angle $\bar{\Phi}$ (counterclockwise counted as positive with 0 and 2π as the trailing edge). Then the following Fredholm equation is numerically solved for the values of γ, the normalized vorticity of the discrete vortices.

$$\gamma(\bar{\Phi}) - \frac{1}{2\pi}\int_0^{2\pi} L(\bar{\Phi}, \psi)\,\gamma(\psi)\,d\psi = \frac{1}{\pi}\int_0^{2\pi} w_n(\psi)\,\dot{s}(\psi)\,\mathrm{cotan}\left(\frac{\psi - \bar{\Phi}}{2}\right)d\psi \qquad (1)$$

In Equation (1), $L(\bar{\Phi}, \psi)$ is an influence coefficient, $w_n(\psi)$ is the normal velocity to the airfoil surface, and $\dot{s}(\psi)$ is the change in distance along the airfoil surface, measured from the trailing edge, with a change in $\bar{\Phi}$. Details of the numerics are contained in Reference 8.

After Equation (1) is solved four times, once for each of the four basic flows mentioned above, the tangential velocity for any point on the airfoil surface may be expressed as a linear sum of the local velocities for each solution:

$$w_t = a w_t^{(1)} + b w_t^{(2)} + c w_t^{(3)} + d w_t^{(4)} \qquad (2)$$

where w_t is the local tangential velocity for separated potential flow solution, $w_t^{(n)}$ is the local tangential velocity computed for basic flow n, and a, b, c, and d are free coefficients to be determined with appropriate boundary conditions.

The coefficients a and b are determined by the free stream velocity, U_∞, and the angle of attack, α:

$$a = U_\infty \cos \alpha$$
$$b = U_\infty \sin \alpha \tag{3}$$

The coefficients c and d are determined by the following two pressure considerations (see Figure 4):

$$p_A = p_B = p_C \tag{4}$$

The condition $p_A = p_B$ is a requirement for constant pressure along the separated free streamline, and the condition $p_B = p_C$ requires that the pressure of the streamline separating from the lower side of the trailing edge be equal, at separation, to the wake pressure.

Once the free coefficients have been evaluated, the potential solution for separated flow from an airfoil is known. However, in determining this solution, it has been tacitly assumed that the location of separation is known. Whether separation actually occurs at the assumed location is determined by a boundary layer calculation using the pressure distribution computed from the potential flow solution described above. When the location of separation predicted by the boundary layer computation agrees with that initially assumed for the potential flow solution, the actual flow about an airfoil with separation has been calculated and thus the values of the force and moment coefficients for the appropriate angle of attack can be determined. In order to conduct the necessary iteration for each solution, Jacob fixes the assumed location of separation and varies the angle of attack until the required agreement between locations of separation is achieved. The manifold of force and moment coefficients is determined by varying the specified location of separation.

Jacob uses boundary layer computation schemes developed by Rotta (see Reference 8 for appropriate reference). Turbulent separation is assumed to occur when the computed shape factor, $H = \delta^*/\theta$, reaches a value of 4.0. According to Sandborn (Ref. 10), this value is too conservative (a more complete discussion of appropriate boundary layer is presented later). Nonetheless, the results obtained by Jacob are impressive. Below is presented a sampling of the results obtained by Jacob.

B. RESULTS OF JACOB'S MODEL

In Figures 5, 6, and 7, there are presented sample results obtained by Jacob (Ref. 8) for NACA 2412 airfoil. Before discussing these results, some observations on Jacob's selection of the NACA 2412 airfoil and the associated data is here appropriate. It should first be noted that the experiments reported by McCullough and Gault (Ref. 1) for a 63_1-012 airfoil section clearly indicated that stall was due to the bursting of a short bubble. Since airfoil thickness has been related to the occurrence of a bubble, one must consider the possibility of the existence of a bubble and its associated influence. Simultaneously, one must also weigh the influence of camber which in this case, may mitigate against the formation of a bubble. The experimental pressure data presented by Jacob, extracted from another reference, is too course for a definitive statement concerning the existence of a bubble. Furthermore, the data was taken from an experiment with a rectangular wing with an aspect ratio of five. With these remarks in mind, comparative results presented by Jacob will now be reviewed.

Figure 5 compares an experimental pressure distribution with that computed by Jacob. The angle of attack was 10.9 degrees and the Reynolds number was 2.7×10^6. The data was taken from an experiment with a rectangular wing with an aspect ratio of five. The agreement is excellent.

In Figure 6, there is presented a comparison of an experimental C_L-α curve with theoretical solutions. While Jacob extracted the experimental data for this comparison from a reference different than that from which he obtained the pressure data, it is suspected that the data refers to the same experiment insofar as the Reynolds number is the same. Furthermore, if one makes the usual correction of the lift curve slope for aspect ratio effects, closer agreement is observed.

Finally, Figure 7 presents a cross plot of $C_{L_{max}}$ vs. Reynolds number. The agreement between theory and experiment is outstanding.

C. POTENTIAL FLOW MODEL FOR HIGH LIFT SYSTEMS

Before considering a potential flow model of a multiple element high lift system with separation, it is important to emphasize here that the salient feature of Jacob's method, discussed above, is the representation of a separated wake by a source flow blockage effect. This feature is readily adaptable to other potential flow methods which heretofore were unable to include separation effects. Thus, it is not necessary for a model of high lift systems to represent the lifting

elements in the manner used by Jacob - a system of discrete vortex elements located on the lifting surfaces. In fact, the potential flow technique of Reference 4 would probably serve as a better basis on which to develop a model of a high system. This preference for the method of Reference 4 is based on the following: (1) that method has been developed for high lift systems without separation, (2) it uses a system of source-sink flows to represent lifting surfaces and thus is consistent with Jacob's potential flow model of the wake blockage effect, and (3) it has already received wide industrial acceptance.

A potential flow model of a high lift system should consist of modeling each lifting element using the method of Reference 4 coupled with the wake blockage model of Jacob. It should be noted that the method of Reference 4 is similar to Jacob's in terms of the superposition of basic flows. It differs from that of Jacob in that, as noted above, source-sink flows are used instead of vortex elements. The strengths of the source-sink surfaces are determined by a simultaneous solution for all the lifting elements located in the desired geometric orientation. This procedure is exactly the same as that currently used in the method of Reference 4 except that an additional basic flow, namely the source wake block flow, must be calculated. The linear combination of the solutions of the basic flows is achieved in the same manner as that established by Jacob and outlined above. However, the boundary condition for the constant pressure wake must now be applied for possibly more than one separated flow region. As with Jacob, the points of separation from the various lifting elements must be specified for the potential flow solution. It is left for a boundary layer calculation to determine the correctness of the specified locations for separation.

SECTION III

BOUNDARY LAYER SOLUTIONS

In order to calculate a "realistic" potential flow solution, a boundary layer computation is necessary to certify that the specified point of separation for the potential solution is indeed the real (correct) location of separation. In order to compute the boundary layer on the suction side of the airfoil, four separate methods are needed to represent the following four types of boundary layer flow: (1) laminar flow from stagnation to transition; (2) transition flow; (3) turbulent flow from transition to approaching separation; and (4) turbulent separating flow. In this section, methods of computation for each of the above listed flows are presented. The described methods were combined and used to calculate an airfoil boundary layer flow for which experimental data was available. A comparison of calculated solution with experimental is presented. Finally, since present methods of computing and predicting separation were inadequate, particular attention was focused on this type of flow and the attendant computation requirements. In the last sub-section of this section there is presented an engineering solution technique developed under this research for the representation of turbulent separation.

A. THE COMPUTATION OF LAMINAR BOUNDARY LAYERS

Before reviewing the method proposed by this research, it is instructive to first examine the objectives of the calculation. For the airfoil flows of interest to this research, there are three possible objectives: (1) the computation of local skin friction; (2) the calculation of velocity profiles for use in a stability analysis for the prediction of transition; and (3) the calculation of laminar boundary layer characteristics at transition. Since skin friction forces are of almost negligible importance in comparison to those due to pressure for lift, drag, and moment calculations, the first objective is of secondary importance, at best. Hence, a high degree of accuracy in the calculation of skin friction is not important for the conditions of interest to this research.

There exist numerous methods for the estimate of the location of transition. The following section provides a discussion of these methods; here it is only of interest to indicate that the use of complex and extensive boundary layer stability calculations, which require accurate evaluation of velocity profiles, are not yet appropriate to this research. Briefly, the justification of this condition rests on the recognition that, not only are the various stability theories inadequately developed to warrant their general application, but, in addition, the

representation of transitional flow is very approximate and thus would overshadow any improvements stability techniques would provide in establishing the location of transition. Therefore, it is not necessary to accurately calculate laminar boundary velocity profiles.

Consequently, the main objective of a laminar boundary layer calculation is to provide an adequate boundary layer representation just prior to transition so that initial conditions can be established for a turbulent boundary layer calculation. Since transition is represented as a change in the shape factor, H, with the momentum thickness, θ, held constant, it is not even necessary to calculate laminar velocity profiles, but, rather, only laminar values of θ and H need be calculated at transition. Therefore, integration of the integral momentum equation,

$$\frac{d\theta}{dx} + (H+2)\frac{\theta}{U}\frac{dU}{dx} = \frac{C_f}{2} \tag{5}$$

is all that is required.

Since Equation (5) contains essentially three dependent variables, θ, H, and C_f, auxiliary equations are necessary. In this research, Thwaites' method (Ref. 3) has been selected for application. Briefly, following Thwaites, Equation (5) may be rewritten:

$$\frac{U}{\nu}\frac{d\theta^2}{dx} = 2\left[\ell(\lambda) - \lambda\{H(\lambda)+2\}\right] \equiv F(\lambda) \tag{6}$$

in which $F(\lambda)$ is assumed to be a universal function of the parameter λ, where λ is defined:

$$\lambda \equiv \frac{\theta^2}{\nu}\frac{dU}{dx} \tag{7}$$

In Equation (6), $H(\lambda)$ and $\ell(\lambda)$ are functional notations for the relationship of the shape factor and skin friction, respectively, with the parameter λ. The function, $\ell(\lambda)$, is related to the skin friction by:

$$C_f = \frac{2\ell(\lambda)}{R_{e_\theta}} \tag{8}$$

where $R_{e_\theta} \equiv \theta U/\nu$.

Thwaites has bound that the following empirical expression can adequately represent $F(\lambda)$:

$$F(\lambda) = 0.45 - 6\lambda \tag{9}$$

Using Equation (9), Equation (6) reduces to the simple quadrature:

$$R_{e_c} (\theta/c)^2 = \frac{0.45}{(U/U_\infty)^6} \int_0^{x/c} \frac{U}{U_\infty} \, d\left(\frac{x}{c}\right) \tag{10}$$

where $R_{e_c} = \frac{U_\infty c}{\nu}$. Once θ is computed from Equation (10), λ is calculated from Equation (7), and $\ell(\lambda)$ and $H(\lambda)$ are determined from a table of values relating λ to those respective functions.

The method of Thwaites described above has received wide acceptance for the calculation of momentum thickness, θ; however, Sandborn (Ref. 10) has raised an objection to the value of H predicted by this method at separation. According to the method described above, laminar separation is predicted at a unique value of λ and, thus, H. Sandborn suggests instead that separation is more accurately predicted by using Equation (10) to predict values of θ, Equation (7) to compute values of λ, and Stratford's (Ref. 11) laminar separation criteria. Consequently, laminar separation may occur for a range of values of H and λ. It should be noted that other methods, such as that of Reference 12, may be used for an adverse pressure gradient near separation.

The interest in the location of laminar separation, and the adverse pressure gradient leading up to it, is primarily due to the concern for the location of transition. Normally, transition is expected somewhere between the suction peak and the location predicted for laminar separation (although laminar separation may not physically occur). At lower lift coefficients, this region can be quite large and thus θ and H can vary over a significantly wide range of values. However, for the conditions of interest to this research, the distance over which transition may occur is very small. Thus, θ does not change significantly, although H may so change. Nonetheless, in the calculations conducted under this research, it has been found adequate to take the suction peak as the location of transition as discussed in the following section. Therefore, it has not been necessary to incorporate the added complexity of a special laminar consideration for the region over which an adverse pressure gradient exists.

The accuracy with which the laminar boundary layer is computed can only be inferred from the comparison of the complete boundary layer calculations with the experimental data of McCullough and Gault (Ref. 1). This comparison is presented in sub-section D. below.

B. THE PREDICTION AND REPRESENTATION OF TRANSITION

Two problems are of interest here: (1) the prediction of the location of transition, and (2) the calculation of the change in boundary layer characteristics through transition.

For the latter problem, the present state-of-the-art provides the following solution technique. First, through the transition region the momentum thickness is assumed constant. That is, it is assumed that transition occurs instantaneously so that the initial value for θ for the turbulent boundary layer equals the laminar value just prior to transition. Next, a change in the shape factor, H, through transition is determined, usually by some correlation curve, Truckenbrodt's (Ref. 13) being the most popular. These correlation curves, such as Truckenbrodt's, relate the Reynolds number based on the momentum thickness at transition to a shape factor change, ΔH. Typically, laminar values of H at transition are of the order 1.8, and turbulent values just after transition are of the order 1.4. Note that only two boundary layer characteristics are calculated through transition. Therefore, if additional information is necessary for a turbulent boundary layer calculation, that information is based on an assumed representative turbulent boundary layer velocity profile which has the proper values of θ and H.

The calculations of this research employed the above discussed representation of transition using Truckenbrodt's correlation curve. In those cases where the momentum thickness Reynolds number was either below or above the range over which the correlation is presented, the minimum or maximum ΔH of the correlation, respectively, was used.

There remains to be discussed methods for the estimate of the location of transition. Stability theories have been under development for many years. Perhaps the best method presently available is that of Reference 14. This method uses the empirical observation that transition occurs when an integrated amplification factor is of the order e^9. Results using this scheme agree very well with experiment. However, the required calculations for application are extensive. Furthermore, as already mentioned, the representation of the changes through transition are of nowhere near equal accuracy.

The method of Reference 15 appears to offer the potential of not only locating transition but, also, describing the changes that occur through transition. While this method may be characterized as a stability theory it is uniquely new and more sophisticated than classical stability theories. However, its development is still in the embryonic stage.

As an alternative, others (Ref. 16 and 17) have suggested the use of transition correlation curves which relate the boundary layer Reynolds number based on the momentum thickness to such other parameters as the Reynolds number based on the distance from stagnation, various shape factors, and the pressure gradient. Generally, if the results of a laminar boundary layer calculation fail to meet anywhere the correlation transition criteria, then the location of transition must be examined from some other standpoint. It should be noted that care must be exercised in the use of such correlations as they are frequently based on restrictive circumstances such as, for example, a particular level of free stream turbulence and/or zero pressure gradient flow. For the calculations of this research program, Michel's method (Ref. 16) was used since a justification for its application to airfoil flows has been established (Ref. 16). However, for the flows considered thus far, Michel's criteria has not been satisifed. Therefore, the following general qualitative approach, suggested in Reference 13, was employed:

1. If Reynolds number is less than approximately 5×10^4 then no transition occurs and the predicted laminar separation physically occurs.
2. For moderate Reynolds numbers (i. e., R_e less than approximately 10^5), transition occurs at the predicted laminar separation point.
3. For Reynolds numbers larger than, say 10^5, transition occurs at the location of minimum pressure.

For all the flows calculated thus far, transition was predicted at the location of minimum pressure.

C. TURBULENT BOUNDARY LAYER SOLUTIONS

In general, many adequate techniques exist for the calculation of turbulent boundary layers on airfoils, except near separation. Near separation, generally all the methods under-predict the variation of the shape factor and the momentum thickness. A discussion of turbulent separating boundary layers, together with a technique developed under this research for the analysis of such boundary layers, is presented later in a sub-section E.

Most of the current methods for the calculation of turbulent boundary layers are presented and compared against both each other and a wide range of experimental data in Reference 18. From that reference, one can select that method which appears to best suit the type of flow under study and which provides the information desired. For the boundary layers of interest to this research, several methods appeared adequate. Head's (Ref. 18) method was selected for the following reasons: (1) it was specifically developed for application to adverse pressure gradient flows; (2) in an earlier comparison of computation schemes (Ref. 19), it was found to best agree with experiment; and (3) it is relatively easy to apply. Below is presented a brief description of this method.

In addition to the integral boundary layer equation, Equation (5), Head derives an additional equation based on the entrainment concept. The continuity equation provides:

$$\frac{d}{dx}\left[U(\delta - \delta^*)\right] = \frac{dQ}{dx} \tag{11}$$

where U, δ, δ^*, and Q are the free stream velocity, boundary layer thickness, displacement thickness, and volume flow rate within the boundary layer, respectively. Head then assumes that the entrainment is determined by the velocity defect in the outer part of the boundary layer which one can think of as being approximately related to some form parameter, such as H, and the free stream velocity, U. Quantitatively, these assumptions may be expressed as:

$$\frac{1}{U}\frac{d}{dx}\left[U\hat{H}\theta\right] = F(\hat{H}) \tag{12}$$

where

$$\hat{H} = \frac{\delta - \delta^*}{\theta} \tag{13}$$

Note that Head uses the form parameter $\hat{H}$ instead of H in quantatizing his assumptions. This was done as a matter of convenience. With the usual assumption of an one-parameter family of velocity profiles, $\hat{H}$ is directly related to H. From this point the success of Head's method depends on empirical expressions for $F(\hat{H})$ and the relationship between H and $\hat{H}$ which best represent experimental data. According to Head's most recent suggestions (Ref. 18):

$$F(\hat{H}) = 0.0306\,(\hat{H}-3)^{-0.653}$$

$$\hat{H} = 1.535(H-0.7)^{-2.715} + 3.3 \qquad (14)$$

In order to complete the system of equations, a representation for the skin friction coefficient, C_f, in Equation (5) must be specified. The Ludwig-Tillman expression

$$C_f = 0.246\,(10)^{-0.678H} R_{e_\theta}^{-0.268} \qquad (15)$$

has been found to be in good agreement with experiment and has been used for all calculations conducted in this research program.

D. COMPARISON OF CALCULATIONS WITH EXPERIMENTAL DATA

In order to assess the ability of the above described methods to represent boundary layers on airfoils with significant separation and to determine where additional development is necessary, a computer program which combined the above methods was developed. This computer program was constructed with a modular format to facilitate easy modification and experimentation. In addition, two other features of the program are worth noting. The transition subprogram provides for five options for the selection of criteria to be used for the determination of the location of transition. This capability was provided for the purpose of experimenting with the various criteria in order to determine their impact on boundary layer calculations. The five options provided are:

1. Use Michel's criteria; if transition is not indicated, use Reynolds number criteria as presented above.
2. Use Michel's criteria; if transition is not indicated, establish transition at location of laminar separation.
3. Use Michel's criteria; if transition is not indicated, establish transition at location of suction pressure peak.
4. Establish transition at location of suction pressure peak.
5. Establish transition at location of laminar separation.

The second feature of note is the incorporation of Stratford's (Ref. 20) criteria for the separation of a turbulent boundary layer. This capability was included for the purpose of determining the applicability of this simple criteria for the flows of interest to this research.

The experimental data of McCullough and Gault were used for comparison with calculations. The experimental pressure coefficient data were used to compute the free stream velocity which otherwise would be provided by a potential flow solution. A discussion of the results of the calculations follows.

Comparisons between calculated and experimental values of the momentum thickness and shape factor are presented in Figure 8 and 9, respectively. These results are also presented for convenience in Tables I and II, respectively. For all cases presented, calculations failed to satisfy Michel's transition criteria. Rather, transition was in all cases established at the suction pressure peak according to the Reynolds number criteria presented above. Transition occurred prior to $x/c = 0.15$.

The results in Figures 8 and 9 show good agreement between theoretical calculations and experiment, except in the vicinity of imminent separation. As a basis of comparison, it should be noted that, at $x/c = 0.15$, the maximum error of the calculated values of θ relative to the experimental values is 8.7 percent, and that the values of H is 3.3 percent. It is, of course, impossible to make a definitive appraisal of the experimental error; however, certain irregularities of the data itself suggest that the disagreement between the calculated values and experimental data is within range of experimental error. It is, nonetheless, interesting to note that the differences, although small, between calculated and experimental data appeared to be systematic, suggesting an error in either or both the measurement technique with its associated data reduction, and the calculation scheme.

The above comparative discussion of the results of boundary calculations does not include the region when the turbulent boundary layer is separating. In this region, the turbulent boundary layer calculation scheme presently being used underpredicts the values of both θ and H. The next section presents a detailed discussion of the problem of representing a turbulent separation, and provides a solution, developed under this research, to this problem. It is here important to note that all other turbulent boundary layer computation schemes also underpredict θ and H at separation.

Before proceeding to a discussion of turbulent separation, two other results obtained from the calculations described above should be mentioned. First, a calculation was made with transition assumed at the predicted location of laminar separation. The results were compared with those for which transition was assumed at the suction pressure peak. The comparisons were presented as Figure 10. For the case presented, the distance between the two assumed transition locations was 1.5 percent of chord. For the case $\alpha = 10$ degrees, this distance increases to only 2.8 percent of chord. As Figure 10 indicates, this small difference in the location of transition produces slight differences in the predicted values of θ and H with a maximum difference of 4 percent in H at separation

where the computation method, in its present form, is not appropriate. Thus, for the flows of interest to this research, the criteria for the prediction of the location of transition is not crucial.

It was mentioned earlier that Stratford's criteria for the separation of a turbulent boundary was also applied to the pressure data of McCullough and Gault. Briefly, Stratford's criteria states that turbulent separation occurs when the following equation is satisfied:

$$(2C_p)^{\frac{1}{4}(n-2)} \left[x \frac{dC_p}{dx} \right]^{\frac{1}{2}} = 1.06\,\beta\,(10^{-6}R)^{\frac{1}{10}} \tag{16}$$

where

$$C_p = \frac{p-p_o}{\frac{1}{2}\zeta U_o^2}$$

$$R = \frac{x U_o}{\nu}$$

$$n = \log_{10} R_s \tag{17}$$

$$R_s = \frac{x_s U_o}{\nu}$$

$$\beta = 0.66 \text{ if } d^2p/dx^2 < 0$$

$$= 0.73 \text{ if } d^2p/dx^2 \geq 0$$

In the above equations the subscript "o" refers to the conditions where the adverse pressure gradient begins, and the subscript "s" refers to the location of separation.

A comparison of the locations of separation predicted by this criteria with experimental data is presented in Figure 11. The locations of separation are presented in terms of the distance, s, from the stagnation point. Thus, s/c, at the trailing edge is greater than one. The experimental location of separation was taken as that point where the shape factor, calculated from Head's method, reached a maximum. The experimental pressure coefficient data was then examined to insure that no anomalies existed. Since the pressure

data stations were five percent of chord apart, and in the interest of fairness in the comparison of Stratford's criteria with experiment, the experimental location of separation is presented in Figure 11 with a ten percent of chord variation. As that figure clearly indicates, Stratford's criteria does not appear well suited to the prediction of turbulent separation of the flows of interest to this research.

E. THE REPRESENTATION AND PREDICTION OF TURBULENT SEPARATION

In the previous section it was indicated that present representations of separating turbulent boundary layers are inadequate. Consequently, attention was directed at this inadequacy and a solution technique was developed to overcome it. For the discussion of this section, the well-known data of Schubauer and Klebanoff (Ref. 21) has been used. This data has been selected over that of McCullough and Gault for the following reasons: (1) the conditions and procedures under which the data of Schubauer and Klebanoff were collected have been more thoroughly documented, and thus regarded as more reliable than the data of McCullough and Gault; (2) Schubauer and Klebanoff's free stream velocity data has been smoothed (see Reference 22) for application to predictor schemes, whereas McCullough and Gault's has not; and (3) McCullough and Gault's data contained several irregularities and thus was less appealing for this study than Schubauer and Klebanoff's data. The smoothed velocity and velocity gradient data of Schubauer and Klebanoff are presented in Figure 12, and experimental values of θ and H are presented in Figures 13 and 14, respectively.

As turbulent separation is approached in the streamwise direction, the following flow characteristics are observed: the boundary layer usually begins to develop an unsteady nature (Ref. 10) other than that normally associated with turbulence, the second derivative of the free stream velocity, d^2U/dx^2, is positive as the pressure coefficient approaches a constant value, and the boundary layer parameters, θ and H, begin to grow at an accelerated rate. Sandborn (Ref. 10) further characterizes a turbulent separating boundary layer as having a time averaged velocity distribution almost the same as that of a laminar boundary layer at separation. In addition, Sandborn establishes a separation criteria which consists of a correlation between H and $\lambda \equiv -(\theta^2/\nu)dU/dx$; however, from the data he presents to substantiate his criteria, it appears that separation can very simply be assumed to have occurred when the shape factor, H, reaches a value between 2.4 and 2.6.

Application of Head's method (described earlier) to Schubauer and Klebanoff's data is shown as the solid lines in Figures 13 and 14.

As noted earlier, that method, as well as others, underpredicted the values of θ and H. While it is recognized that the integral momentum equation is not strictly valid in the vicinity of separation since it is based on boundary layer assumptions which, in this case, are not satisfied, it is of interest to examine each of the terms in this equation.

In Reference 22 there is presented skin friction data based on a fit of the "law of the wall" velocity distribution. In addition, there is also presented the predicted skin friction values based on the Ludwig-Tillman correlation. The agreement between the values of C_f computed from these two independent methods is acceptable. Substitution of experimental values of θ, H, U, and dU/dx into the left-hand side of Equation (5) leads to the observation that the magnitude of dU/dx is too low. This is not to suggest that the experimental data is in error, but, rather, a more negative value of dU/dx is necessary to balance the boundary layer integral equation, in this case, Equations (5) and (15). The intent of this discussion is to indicate a systematic way in which the momentum integral equation may be modified for application to turbulent separation.

Before pursuing this discussion, some observations concerning the pressure distribution near separation are appropriate. It should first be noted that, for airfoil type flows, in the immediate vicinity of separation the second derivation of the pressure gradient, d^2p/dx^2 becomes strongly positive (see Figure 12b for an indication of this phenomenon). It has been further observed in the calculations of this research that the predicted values of θ and H, such as obtained with Head's method, begin to deviate from experiment when the pressure begins to change as just described. Finally, calculation schemes such as that due to Head will accurately predict the location of separation and the boundary layer characteristics if a constant pressure gradient is used instead of, and over the region where, the pressure gradient decreases to zero. In fact, it is interesting to note that the potential flow solution of Jacob (see Figure 5) does not predict a continuous variation of dp/dx in the region of separation. It is, therefore, postulated that the integral momentum equation can be accurately used for the calculation of separation if the velocity gradient, dU/dx, is based on a pressure gradient consistent with a potential flow predicate for the region where the boundary layer is separating. As a temporary local assumption, that pressure may be taken as constant.

Note here that separation is described as occurring in a "region" (i. e., streamwise distance) instead of at a point. This description is not only completely consistent with Sandborn's representation of turbulent separation, but, in fact, is based on it. In the

case of Schubauer and Klebanoff's data the separation region is between the points labeled "a" and "b" in Figures 12, 13, and 14.

There needs yet to be described the connection between the experimental pressure distribution and the indicated required constant pressure gradient. Further, this constant pressure gradient must be associated with potential flow calculations. Before passing to this latter task, the former problem will first be resolved with the use of Schubauer and Klebanoff's data.

As noted earlier, the inability of the integral momentum equation, Equation (5), to represent separation is fundamentally based on the fact that the Prandtl type boundary layer assumptions are not satisfied near separation. The departure from boundary assumptions may be related to the magnitude of $d\delta^*/dx$ since, from an order-of-magnitude consideration:

$$\frac{V}{U} = \frac{d\delta^*}{dx} \tag{18}$$

where V and U are representative values of the transverse and streamwise velocities, respectively. The following representative order-of-magnitude values of V/U are presented to serve as a basis of comparison for the various types of boundary layer flow:

$0\left[\frac{V}{U}\right]$	= 0.00085	flat plate laminar flow
	= 0.0037	flat plate turbulent flow (based on 1/7 velocity profile)
	= 0.006	adverse pressure gradient turbulent flow prior to separation (from Schubauer and Klebanoff's data)
	= 0.05-0.2	turbulent separation region (from Schubauer and Klebanoff's data)

where 0[ ] means "order-of-magnitude". Note that while the values of V/U for non-separating turbulent flow are of the order-of-magnitude of 10 greater than the value appropriate to laminar flow, they are also a factor of 10 to almost 100 less than the values consistent with turbulent separation.

With the recognition that the boundary layer growth rate for turbulent separation is inconsistent with boundary layer assumptions, $d\delta^*/dx$ is taken as a correlating parameter. The constant pressure

gradient is then related to the experimental pressure gradient by:

$$\left[\left(\frac{dp}{dx}\right)_f - \left(\frac{dp}{dx}\right)_e\right] = G\left(\frac{d\delta^*}{dy}\right) \tag{19}$$

where $G(\frac{d\delta^*}{dy})$ is hypothesized to be a universal function, and the subscripts "f" and "e" refer to the fictious constant pressure gradient and the experimental pressure gradient, respectively.

The concept of using a constant pressure gradient in the separation region was applied to Schubauer and Klebanoff's experiment where the value of the constant pressure gradient was taken as that at point "a" of Figure 12b, and Head's computation scheme was used. The results computed with this approach are shown as the dashed line in Figured 13 and 14. As can be seen from the figures, the predicted values of θ agree very well with experiment and the predicted values of H are within ten percent of experiment. The explanation for the error in the computed values of the shape factor rest in the recognition that the family of velocity profiles associated with Head's method is slightly different than that associated with a separating boundary layer. Sandborn (Ref. 10) has identified the correct family of velocity profiles consistant with separation.

The function $G(d\delta^*/dx)$ can be readily determined from any set of experimental data. However, it should be noted that the form of Equation (19) is not suitable as a general expression since it has a dimensional character. Thus, Equation (19) should be regarded as a conceptual expression that must be generalized.

Some additional comments on the application of the above described method to experimental data and potential flow solutions is in order. The decision to apply the above described correction to the integral momentum equation in any given calculation should be made based on two criteria: (1) the value of $d\delta^*/dx$ is greater than a certain minimum value (present indications are that this minimum is 0.02), and (2) the second derivative of the pressure gradient is positive. Both criteria should be satisfied simultaneous. The first criteria, as noted above, is an indication that boundary layer assumptions are becoming unappropriate. The second criteria, in conjunction with the first, determines the location where the suggested modifications should begin. With regard to applications based on experimental pressure distributions, it may not be appropriate to define the fictitious pressure gradient as a constant when the wall radius-of-curvature is small. In the case of Schubauer and Klebanoff's data the wall radius-of-curvature was large, and, thus, a constant fictitious pressure gradient

was used as an approximation. In any case, whether the wall radius is small or large, the approach suggested above should use as the fictitious pressure gradient that determined from a potential flow solution which incorporate the flow field effect of separation.

The fundamental concept of method proposed herein can, therefore, be seen as follows. Experimental pressure distributions deviate from those computed from a potential flow solution with separation because of the rapid growth of the displacement thickness, δ^*, which significantly alters the effect shape of the body. Simultaneously, the rapid increase in δ^* invalidates the usual boundary layer assumptions. However, as far as boundary layer calculations are concerned, the potential flow pressure distribution is appropriate provided the change in the shape of the velocity distribution, as provided by Sandborn, is taken into account. The actual pressure distribution may be recovered from the potential solution through a correlation based on $d\delta^*/dx$. Thus, the connection between experimental and potential flow pressure distributions is achieved. In the light of the above discussions, it is interesting to note that the pressure coefficient at separation, and thus in the wake, computed by Jacob (Figure 5) is slightly higher than experiment - a condition anticipated by development presented herein. It should, further, be recognized that, while inaccuracies in the predicted wake pressure have only a small influence on lift coefficients computed from pressure distributions, those same inaccuracies have a much stronger effect on the prediction of moment coefficients.

It has been noted above that Equation (19) represents the conceptual form of the correlation between the experimental and potential flow pressure distributions in the turbulent separating flow region. In order to establish an operational form for this correlation, both the data of Schubauer and Klebanoff (Ref. 21) and the data of McCullough and Gault (Ref. 1) have been used. It was believed that these two sets of data are sufficiently different that any correlation which adequately represents both sets of data should be representative of all separating flows from airfoil sections. It should, however, be noted here that only that data from McCullough and Gault for separating flow from the NACA 63_3-018 airfoil at twelve degrees angle-of-attack has presently been employed.

From the above referenced data, the operational form of the correlation is:

$$(R_e \times 10^{-6})^{1.4}\left[\left(\frac{dC_p}{dx}\right)_f - \left(\frac{dC_p}{dx}\right)_e\right] / \left(\frac{dC_p}{dx}\right)_f = G_1\left(\frac{d\delta^*}{dx}\right) \qquad (20)$$

where

$$R_e = \frac{u_r x_r}{\nu} ,$$

$$C_p = \frac{p - p_r}{q_r} ,$$

and where u_r is the velocity at the start of the separating flow region (point "a" in Figure 12) and x_r is the distance measured from that same location. The function G_1 is presented as Figure 15. In that same figure there are presented experimental values computed from the above cited data with the aid of Equation 20.

Several observations are here appropriate. In developing Equation (20), a considerable amount of smoothing of experimental data was necessary. From the smoothed data, the appropriate derivatives were computed by a first order difference procedure. Naturally, reducing experimental data in this fashion introduces some degree of variation between the experimental data and the results from smoothed functions. Furthermore, the accuracy of original data is itself unknown. The correlation, Equation (20), and its future application is dependent upon the accurate determination of the location where separation begins to occur. In this work that location was specified where $d\delta^*/dx = 0.02$. In terms of experimental data, this location usually falls between data stations, requiring interpolation with associated errors. Finally, it has been found that the exponent of the Reynolds number in Equation (20) has a slight dependence on a Reynolds number based on the length of the separation region. Specifically, that exponent, now represented by N, appears to be related to $R_{e_s} = u_r \ell_s / \nu$ as follows:

$$N = \frac{1}{a} (\eta - 2) \qquad (21)$$

where

$\eta = \log_{10} R_{e_s}$

ℓ_s = length of the separation region

a = of the order of magnitude of 3.5.

However, the work here presented is insufficient to establish the precise relationship. Nonetheless, in view of the above comments, the correlation, Equation (20), presented as Figure 15 does a remarkable job of representing two very different sets of experimental data.

SECTION IV

CONCLUSIONS AND RECOMMENDATIONS

The necessary and appropriate analytic-empirical methods have been identified and developed for application to the prediction of the performance of high lift systems where the nonlinear effects of flow separation exert a significant influence. While the various methods have been applied to the study of a single airfoil section, a procedure for the development of a potential flow model for multiple element high lift systems has been outlined. There remains the actual construction of the computer program for the simulation of such systems. Such an effort is here strongly recommended.

The viscous flow computation techniques identified and developed in this work apply to each element of a multiple element high lift system. However, additional observations are here appropriate. When separation occurs from more than one element, some consideration of the mixing along separated streamlines is important. The determination of whether such mixing reaches a boundary layer on a downstream element is of very great importance and proper consideration should be given to the combining turbulent viscous flows when such circumstances do occur. A number of classical methods (Reference 23) for computing the mixing along free streamlines exist. The mixing of a free mixing region and a turbulent boundary layer may be computed using the well known method of Reference 24. However, before expending a great effort in this area, a model, high lift system which does not include the consideration just mentioned, should be developed from which the relative importance of the interaction of free mixing with a boundary layer may be determined. Moreover, it will also be important to determine the relative importance of wakes from elements from which the flow does not separate. From studies with models which do not include these various effects, one is in a sound position to provide any additional effort necessary to resolve any demonstrated problem areas.

Finally, it should be noted that the turbulent separating flow model developed in this work, and discussed in the previous section, would be adequate for application in its present form. Nonetheless, the correlation should be compared with additional data and the relationship between the empirical exponent and the Reynolds number should be more precisely determined.

REFERENCES

1. McCullough, G. B., and D. E. Gault, "Examples of Three Representative Types of Airfoil-Section Stall at Low Speed," NACA TN 2502, 1951.

2. Abbott, I. H. and A. E. von Doenhoff, Theory of Wing Sections, Dover Publications, Inc., New York, 1959.

3. Thwaites, B., ed., Incompressible Aerodynamics, Oxford Press, 1960.

4. Hess, J. L. and A. M. O. Smith, "Calculation of Potential Flow About Arbitrary Bodies," Progress in Aeronautical Sciences, Vol. 8, Pergamon Press, 1967.

5. Mavriplis, F., "A Vorticity Distribution Method for Calculating Two-Dimensional Potential Flow about Arbitrary Multi-Element High Lift Airfoils," Canadair Report No. ERR-RAZ-000-303.

6. Jacob, K. and F. W. Reigels, "The Calculation of the Pressure Distribution over Aerofoil Sections of Finite Thickness with and without Flaps and Slats," Zeitschrift für Flugivissenschaft, Part 9, 1963, RAE Library Translation 11, 1965.

7. Hancock, G. J., "Problems of Aircraft Behavior at High Angles of Attack," Agardograph 136, April, 1969.

8. Jacob, K., "Computation of Separated Incompressible Flow Around Airfoil and Determination of Maximum Lift," Translation of abbreviated version of "Theoretische Berechnuncy von Druckverteibing und Kraftbeiwerten für beliebige Profile bei inkompressibler Strömung mit Ablösung," Bericht 67A62 der Aerodynamischen Versuchsanstalt Göttingen, 1967. Translation is STAR accession no. N69-29623.

9. Hurley, F. X., "Airfoil Pressure Distributions in Low Speed Stall," McDonnell Douglas, McDonnell Research Laboratories Report H184, St. Louis, Mo., April, 1969.

10. Sandborn, V. A., "Characteristics of Boundary Layers at Separation and Reattachment," Research Memorandum CEM 68-69VAS14, College of Engineering, Colorado State University, February 1969. See also J. of Fluid Mech., Vol. 32, Part 2, pp. 293-304, 1968.

11. Stratford, B.S., "Flow in the Laminar Boundary Layer Near Separation," ARC R&M 3002, 1957.

12. Smith, A.M.O. and D.W. Cutter, "Solution of the Incompressible Laminar Boundary Layer Equations," AIAA J., Vol. 3, No. 4, April, 1963, pp. 639-647.

13. Schlichting, H., Boundary-Layer Theory, McGraw Hill Book Co., New York, 6th ed., 1968.

14. Jaffee, N.A., T.T. Okamura and A.M.O. Smith, "Determination of Spatial Amplification Factors and Their Application to Predicting Transition," AIAA J., Vol. 8, No. 2, February 1970.

15. Raetz, G.S., "A Hypothetical Model of a Transitional Boundary Layer," AFFDL-TR-70-123, November 1970.

16. Smith, A.M.O. and N. Gamberani, "Transition, Pressure Gradient and Stability Theory," Douglas Aircraft Co., Report No. ES 26388, El Segundo, Calif., August 1956.

17. Miley, S.J., "The Design of Airfoils for Low Reynolds Number Flight," Paper presented at the Conference on V/STOL Oriented Research, Illinois Institute of Technology, April 1970.

18. Kline, S.J., M.V. Morkovin, G. Sovran and D.J. Cocknell, ed., Proceedings: Computation of Turbulent Boundary Layers - 1968 AFOSR-IFP - Stanford Conference, Vol. I, Thermosciences Division, Dept. Mechanical Engineering, Stanford University, Calif., 1969.

19. Thompson, B.G.J., "A Critical Review of Existing Methods of Calculating the Turbulent Boundary Layer," ARC R&M 3447, 1967.

20. Stratford, B.S., "The Prediction of Separation of the Turbulent Boundary Layer," J. of Fluid Mech., Vol. 5, Part 1, 1959.

21. Schubauer, G.B. and P.S. Klebanoff, "Investigation of Separation of the Turbulent Boundary Layer," NACA TN 2133, 1950.

22. Coles, D.E. and E.A. Hirst, Eds., Proceedings: Computation of Turbulent Boundary Layers - 1968 AFOSR-IFP - Stanford Conference, Vol. II: Compiled Data, Thermosciences Division, Department of Mechanical Engineering, Stanford University, Calif., 1969.

23. Harsha, P.T., "Free Turbulent Mixing: A Critical Evaluation of Theory and Experiment," AEDC-TR-71-36, February 1971.

24. Bradshaw, P., Ferris, D.H. and Atwell, N.P., "Calculation of Boundary-Layer Development Using the Turbulent Energy Equation," J. Fluid Mech., Vol. 28, Part 3, pp. 593-616, 1967.

TABLE I

VALUES OF MOMENTUM THICKNESS, $\theta/c \times 10^3$

α =	10°		12°		13°		14°		15°	
x/c	CAL.	EXP.	CAL.	EXP.	CAL.	EXP.	CAL.	EXP.	CAL.	EXP.
.15	.459	.450	.498	.533	.530	.576	0.555	0.586	.573	.630
.20	.583	.542	.635	.634	.681	.683	0.716	0.726	.758	.775
.25	.687	.610	.757	.722	.809	.784	0.873	0.828	.946.	.915
.30	.819	.751	.908	.867	.980	.939	1.082	1.061	1.238	1.114
.35	.915	.920	1.064	1.065	1.157	1.162	1.332	1.317	1.652	1.613
.40	1.118	1.060	1.263	1.259	1.408	1.361	1.718	1.501	2.264	1.690
.45	1.339	1.211	1.533	1.419	1.748	1.617	2.285	1:937	2.744	2.562
.50	1.621	1.598	1.881	1.927	2.225	2.329	2.877	3.438		
.55	1.943		2.311		2.812					
.60	2.392	2.373	2.770	2.901	3.416	3.395				
.65	2.877	2.857	3.525	3.772	3.840	5.428				
.70	3.492	3.588	4.191	4.630						
.75	4.019	3.981	4.688	5.433						
.80	4.669	4.901	5.031	7.002						
.85	5.293									
.90	5.889	7.022								

TABLE II

VALUES OF SHAPE FACTOR, H

α =	10°		12°		13°		14°		15°	
x/c	CAL.	EXP.	CAL.	EXP.	CAL.	EXP.	CAL.	EXP.	CAL.	EXP.
.15	1.48	1.44	1.50	1.48	1.52	1.50	1.54	1.50	1.55	1.50
.20	1.47	1.47	1.49	1.52	1.52	1.53	1.53	1.53	1.55	1.54
.25	1.46	1.45	1.48	1.47	1.50	1.49	1.53	1.51	1.56.	1.52
.30	1.47		1.49	1.50	1.51	1.52	1.55	1.53	1.61	1.55
.35	1.47	1.48	1.50	1.49	1.52	1.50	1.57	1.56	1.69	1.67
.40	1.48	1.52	1.52	1.54	1.55	1.56	1.65	1.60	1.85	1.65
.45	1.51	1.55	1.55	1.59	1.61	1.63	1.77	1.75	1.89	1.92
.50	1.55	1.55	1.60	1.64	1.69	1.69	1.88	1.94		
.55	1.59		1.67		1.80					
.60	1.66	1.72	1.73	1.84	1.89	2.00				
.65	1.72	1.78	1.87	2.00	1.89	2.20				
.70	1.82	1.91	1.96	2.18						
.75	1.86	1.86	1.98	2.14						
.80	1.94	2.12	1.93	2.46						
.85	1.99									
.90	2.03	2.326								

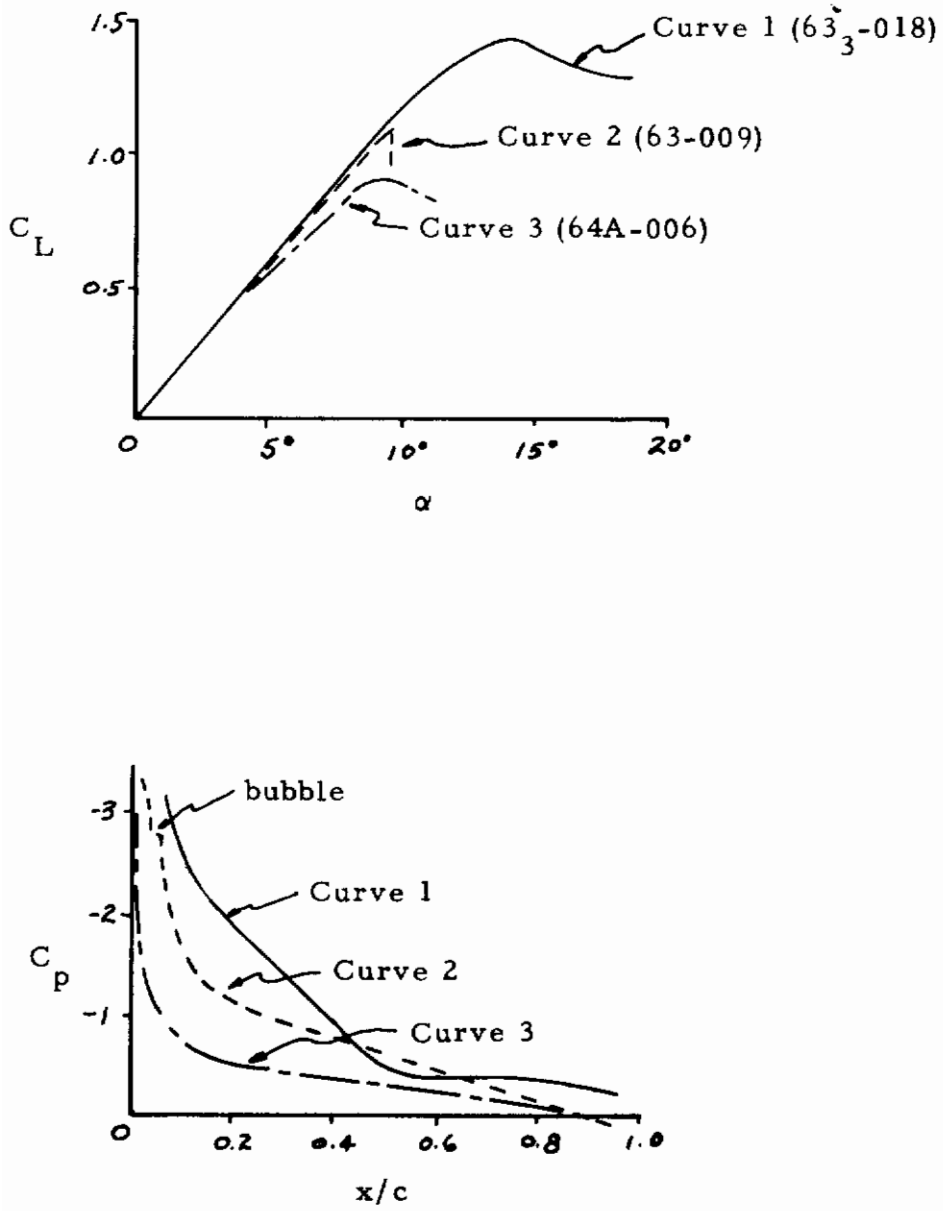

Figure 1. Comparisons of Lift Curves and Pressure Distribution for Three Different Airfoils (from Reference 1).

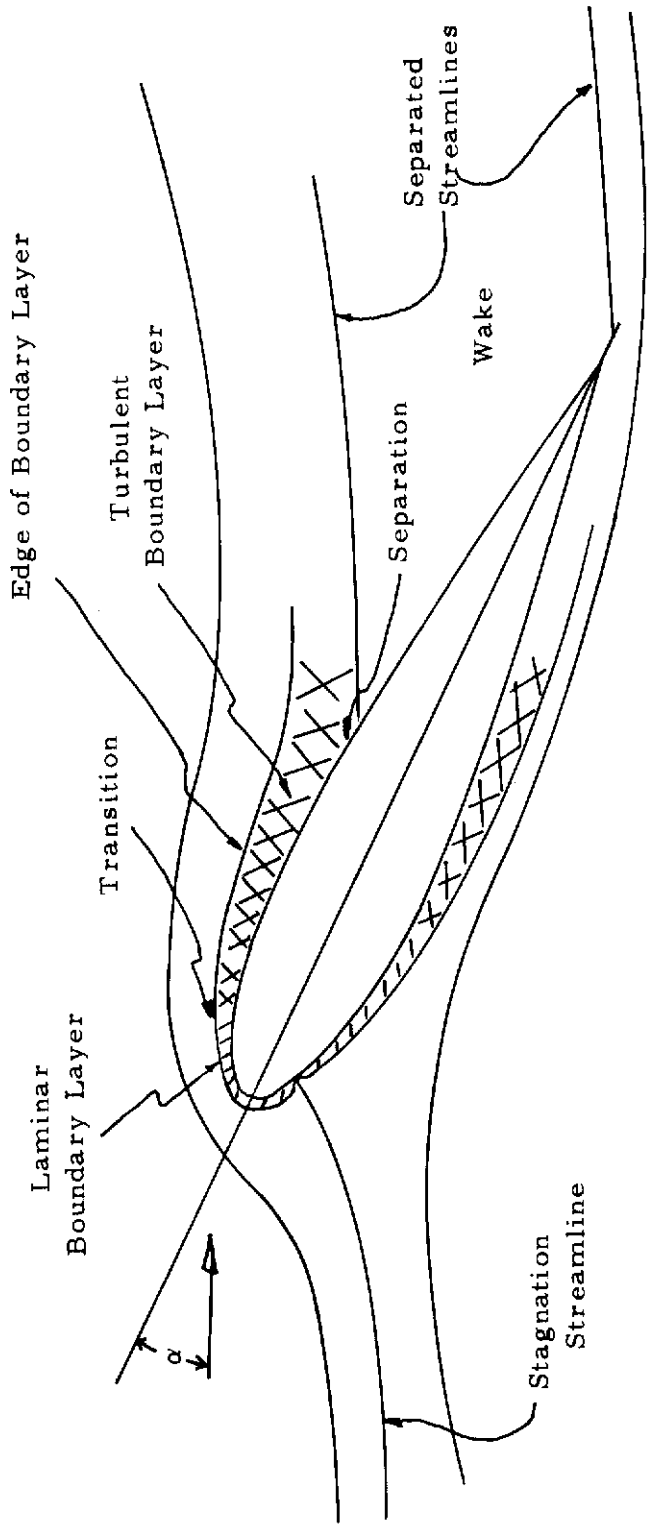

Figure 2. Exaggerated Sketch of Relevant Basic Flow Phenomena.

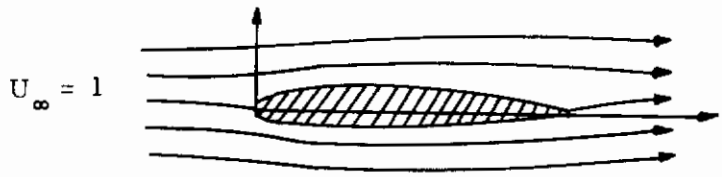

(a)

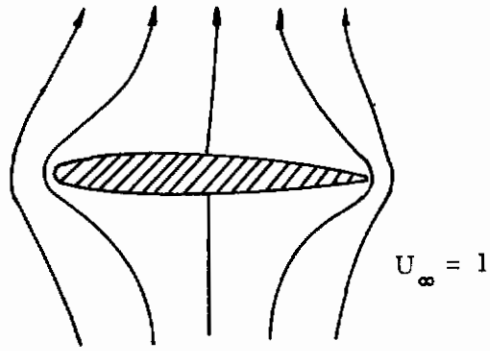

(b)

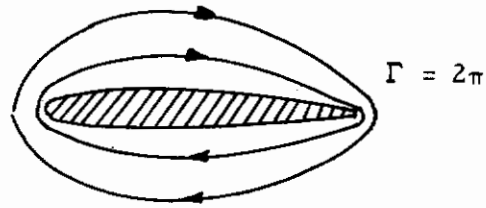

(c)

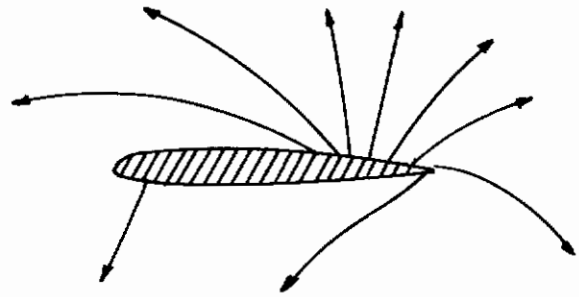

(d)

Figure 3. Basic Solutions for Synthesis of Separated Potential Flow.

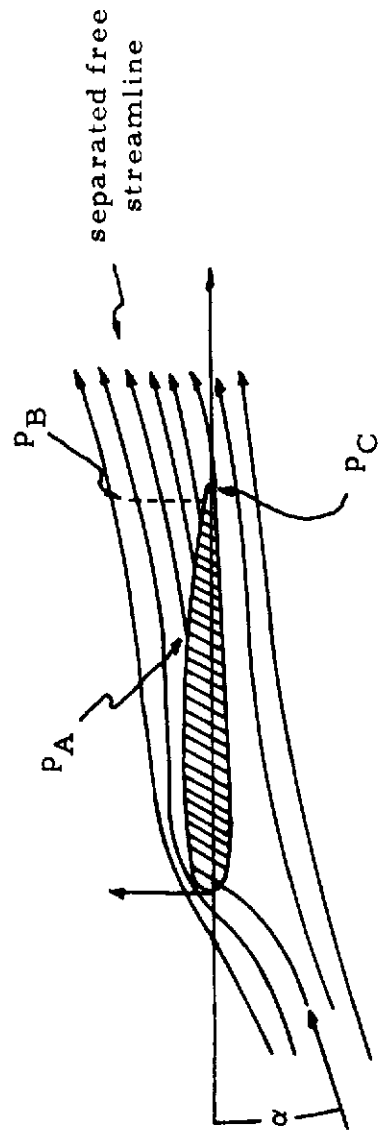

Figure 4. Synthesized Separated Potential Flow.

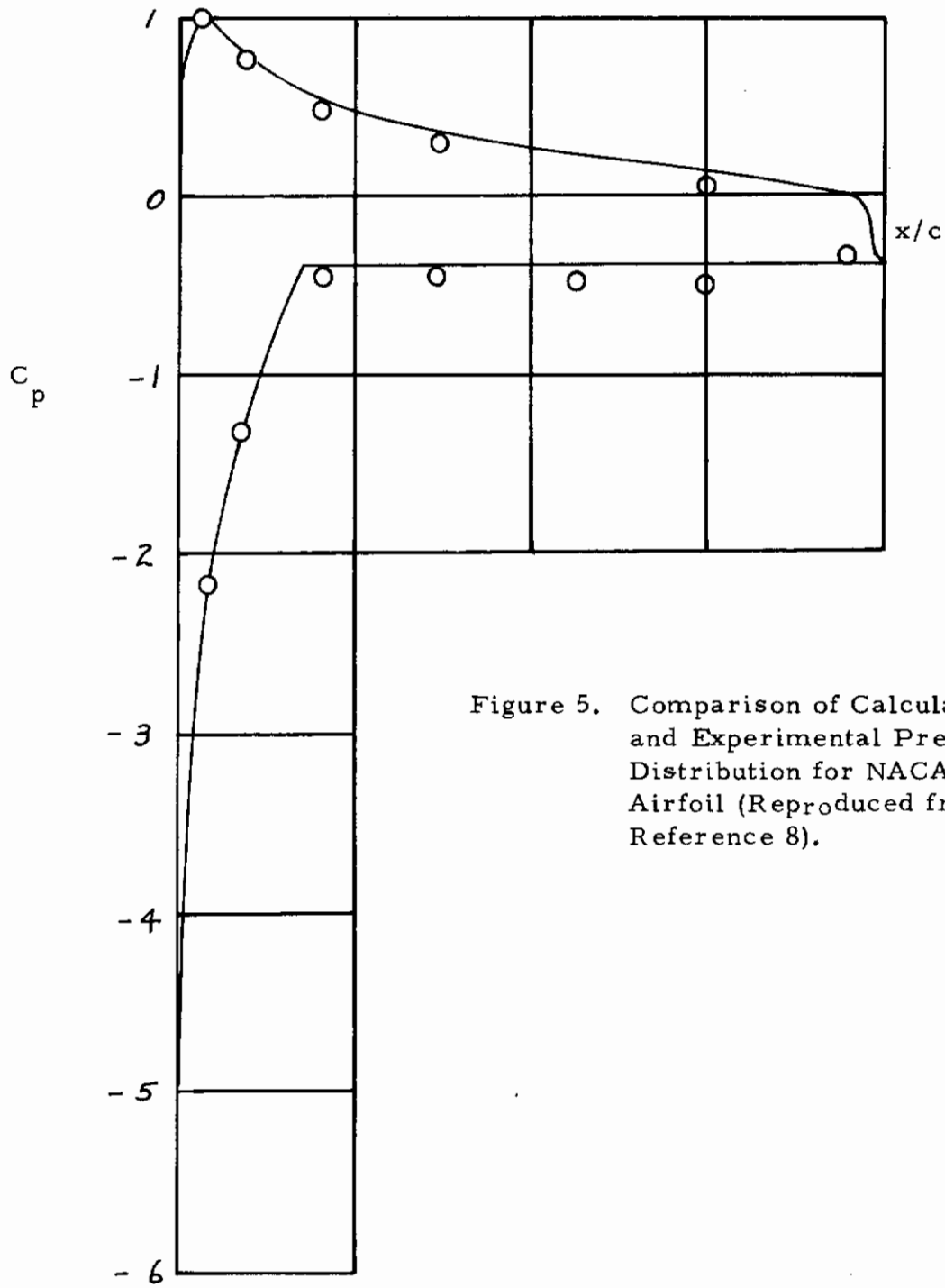

Figure 5. Comparison of Calculated and Experimental Pressure Distribution for NACA 2412 Airfoil (Reproduced from Reference 8).

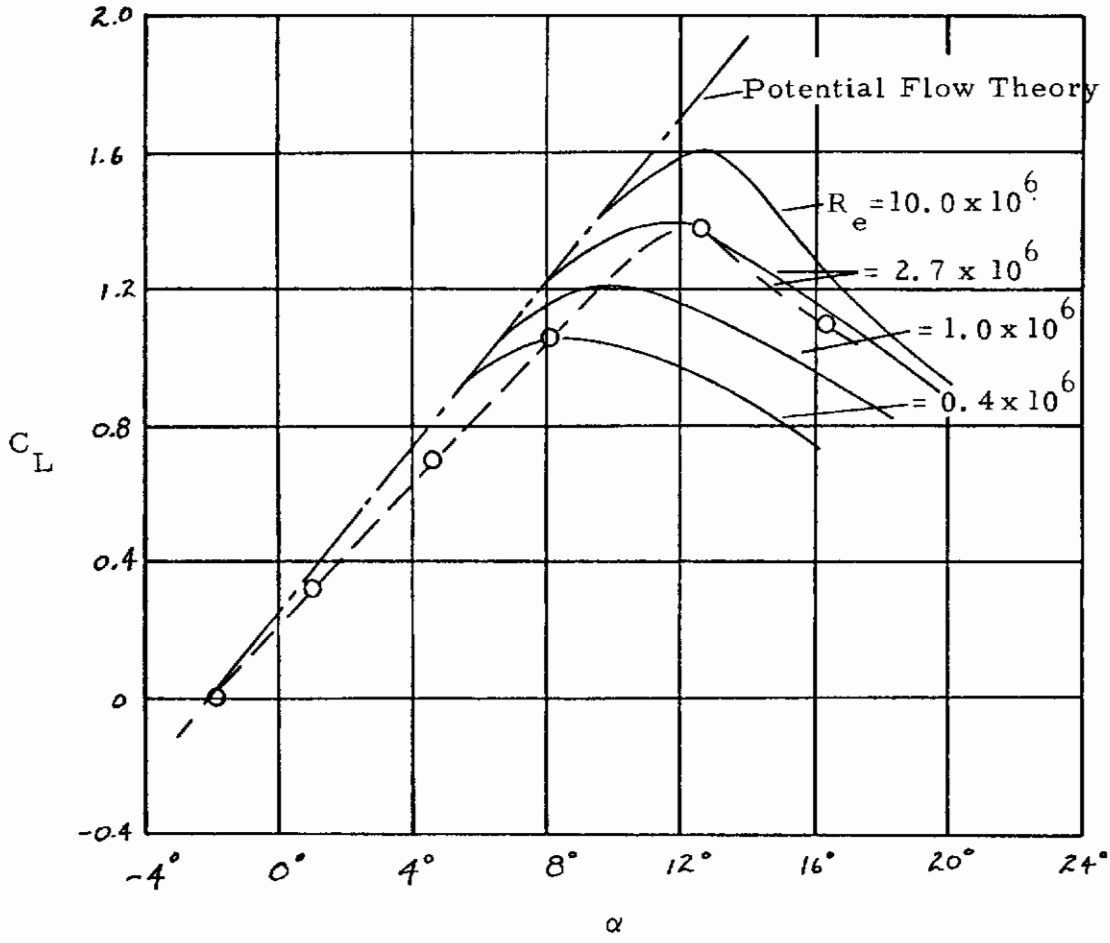

Figure 6. Comparison of Calculated and Experimental Lift Coefficient versus Angle-of-Attack for NACA 2412 Airfoil (Reproduced from Reference 8).

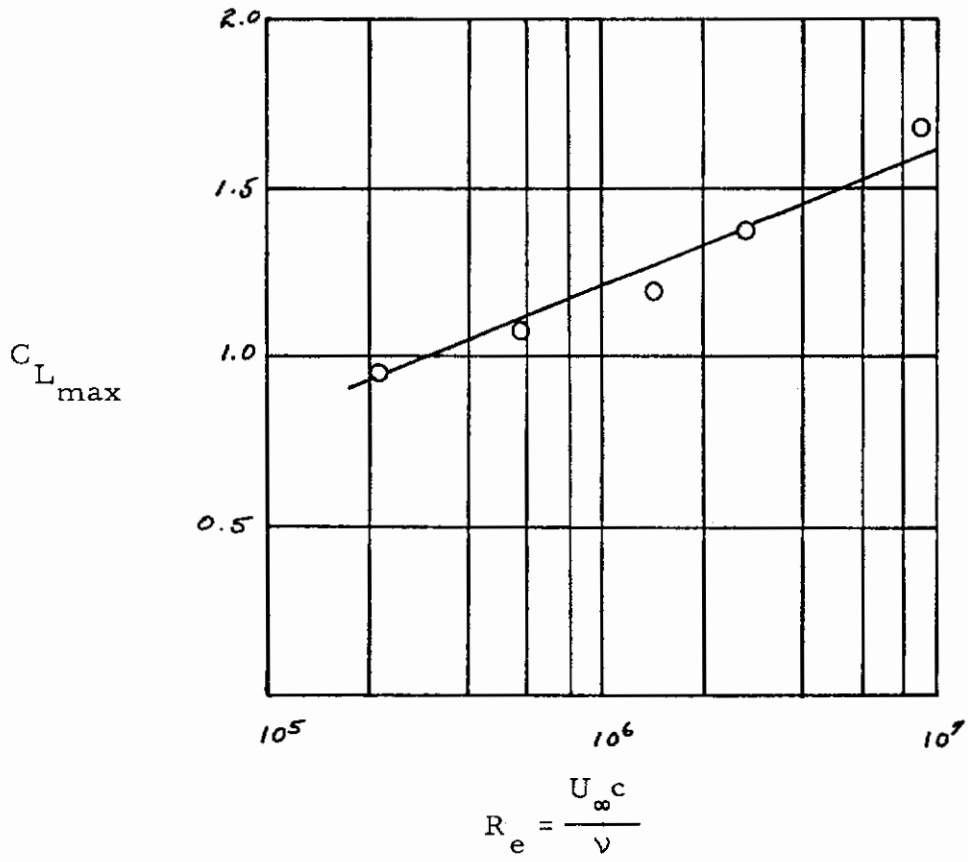

Figure 7. Comparison of Calculated with Experimental Maximum Lift Coefficient as a Function of Reynolds number for NACA 2412 Airfoil (Reproduced from Reference 8).

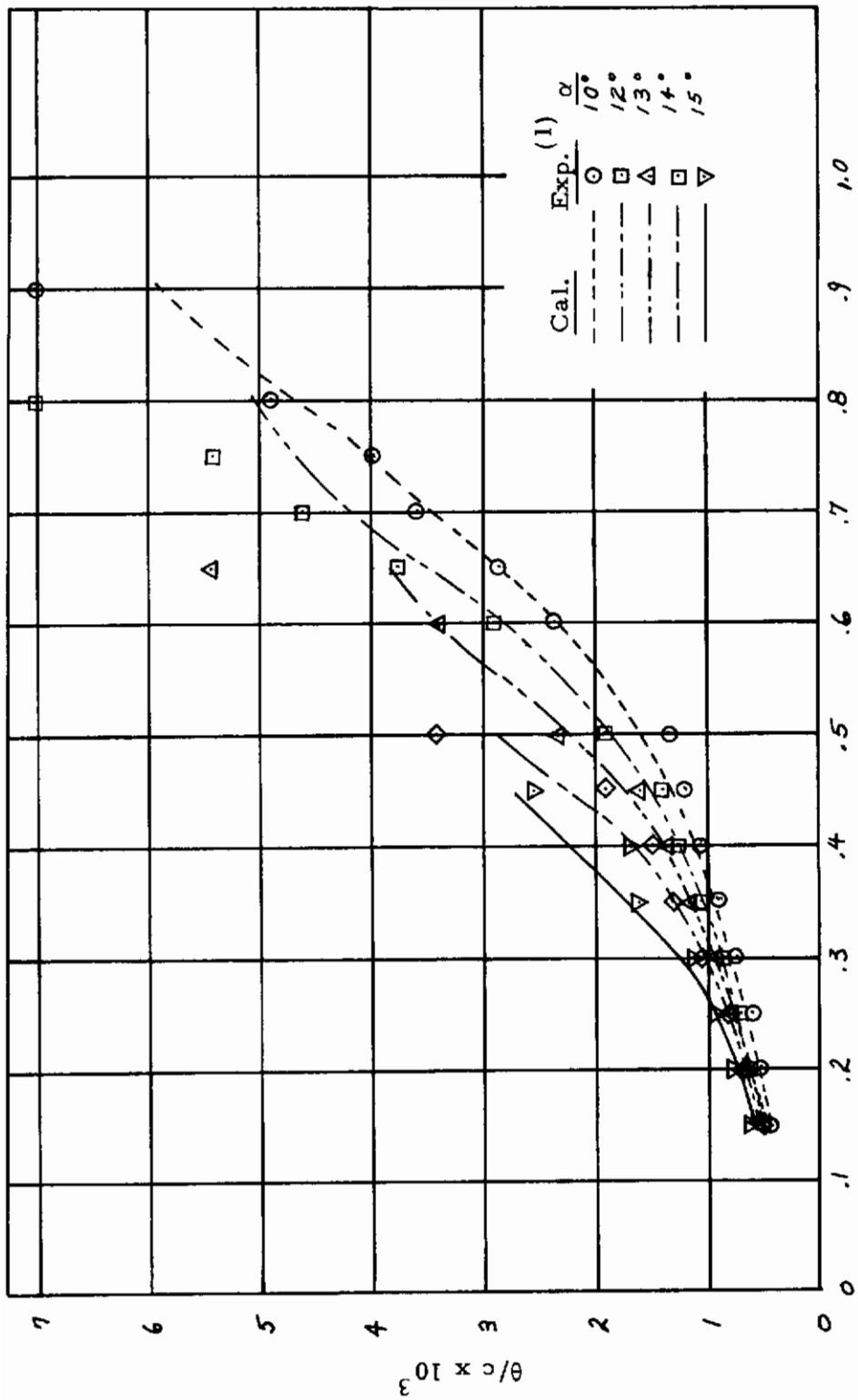

Figure 8. Comparison of Calculated with Experimental Values of the Momentum Thickness for NACA 63_3-018 Airfoil.

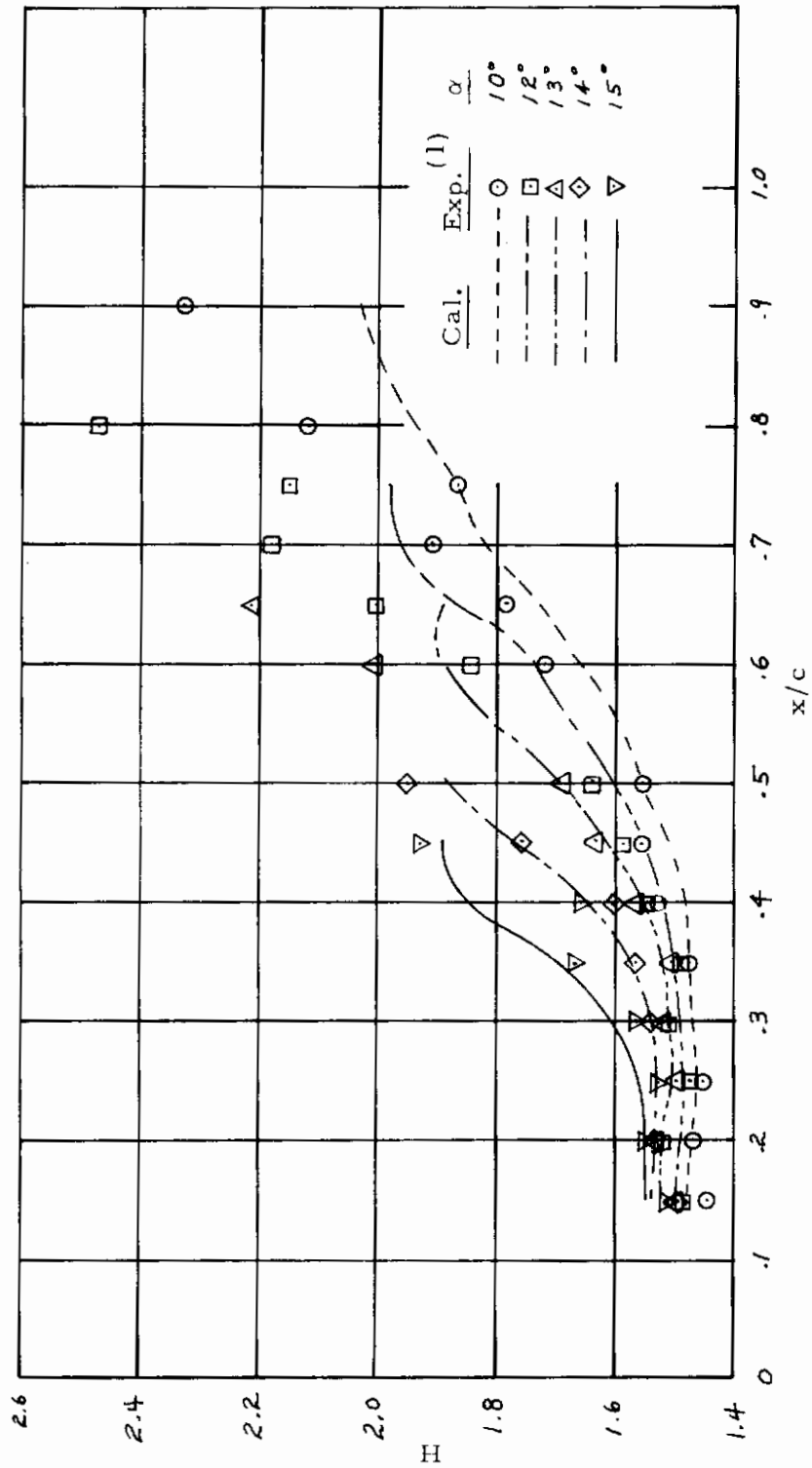

Figure 9. Comparison of Calculated with Experimental Values of the Shape Factor for NACA 63_3-018 Airfoil.

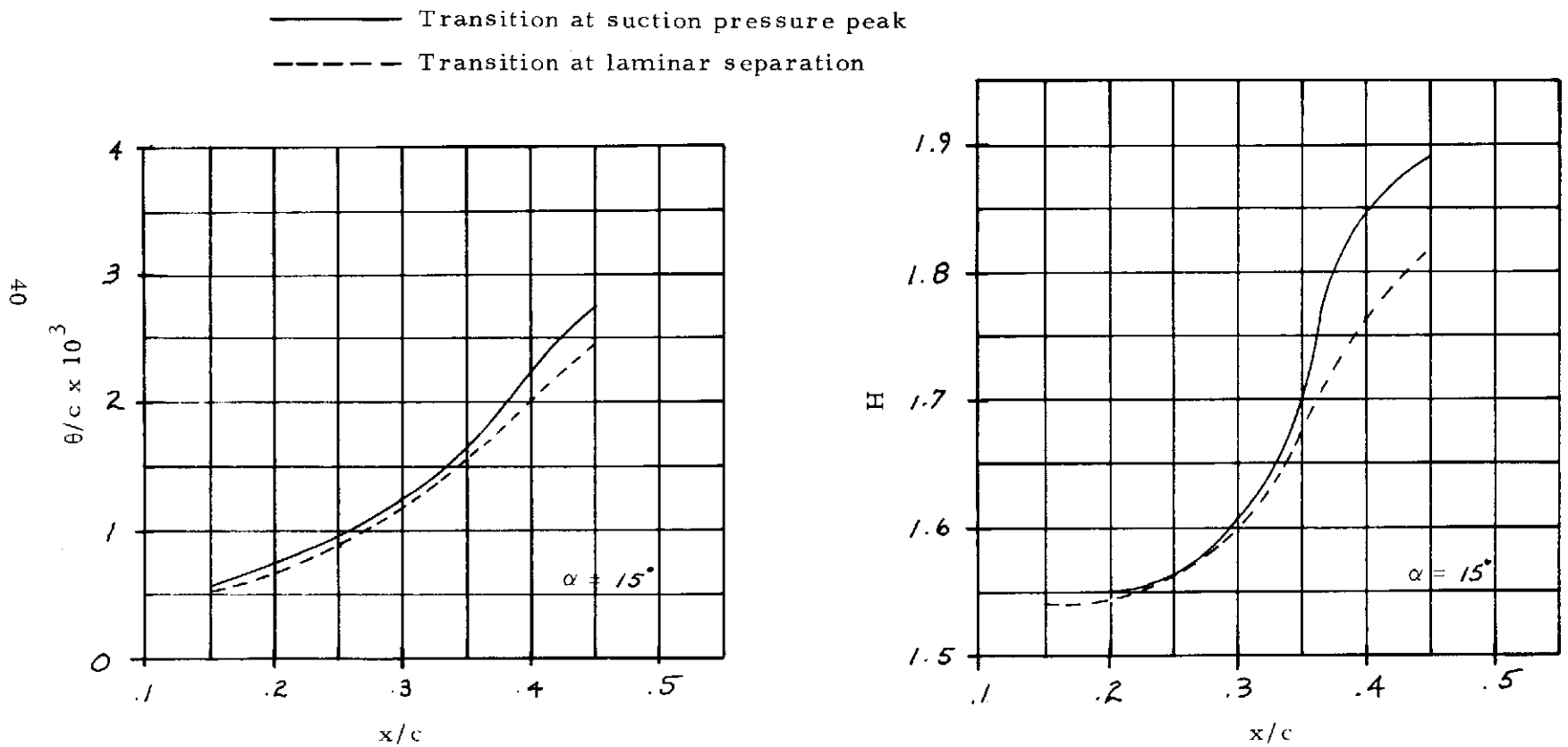

Figure 10. Comparison of the Effect of the Assumed Location of Transition.

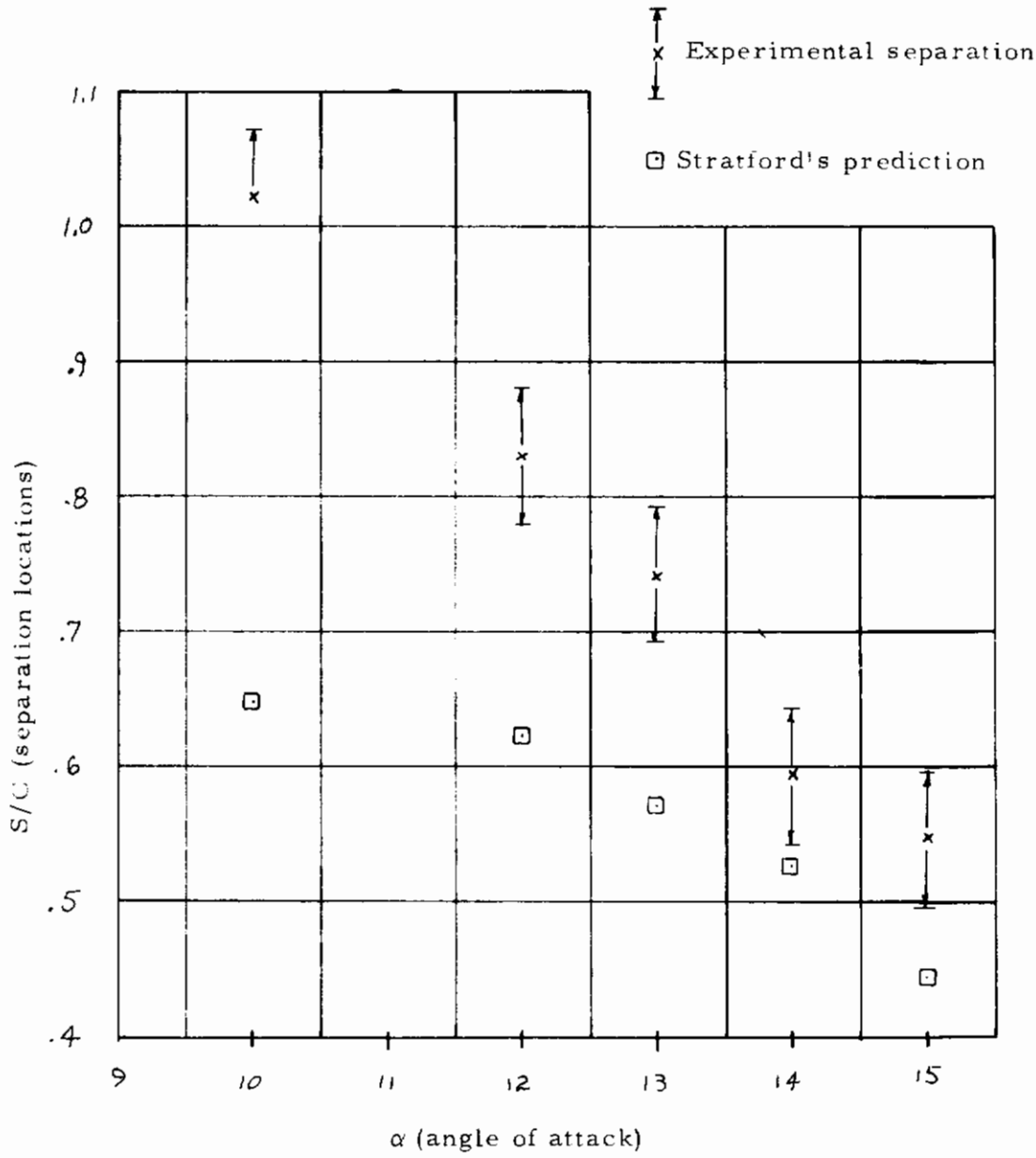

Figure 11. Comparison of Stratford's Criteria[20] for the Prediction of Separation.

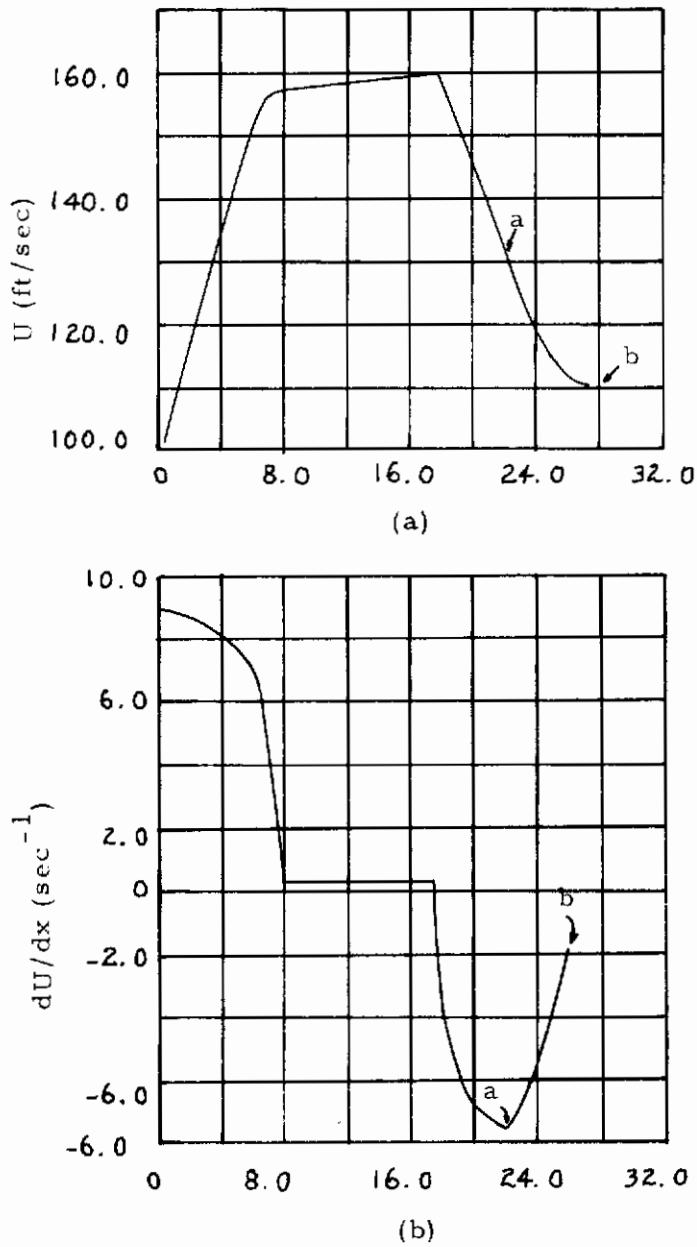

Figure 12. Smoothed Distributions of U and dU/dx for Schubauer and Klebanoff's data (Reproduced from Reference 22).

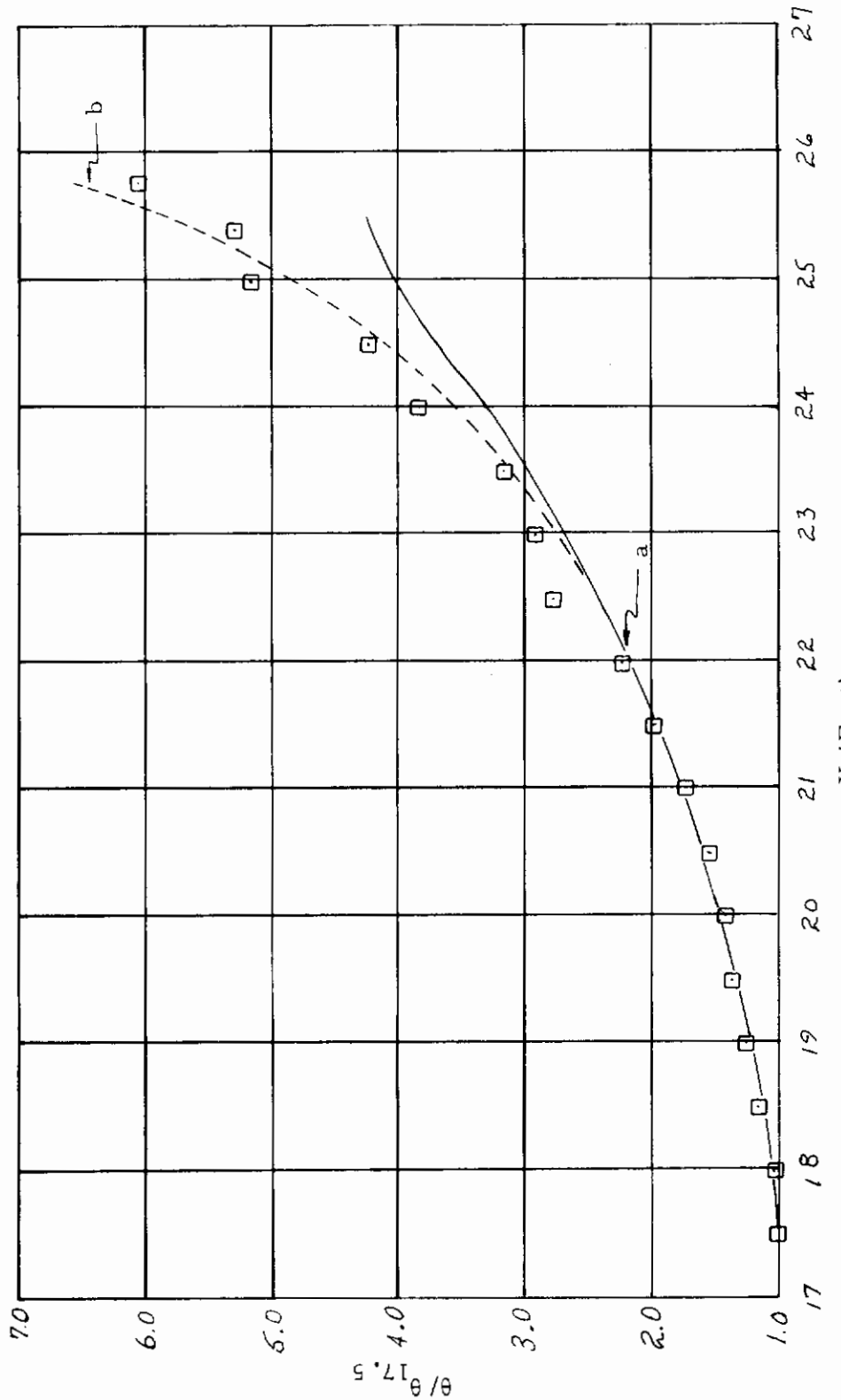

Figure 13. Comparisons of Calculations with the Data of Schubauer and Klebanoff.

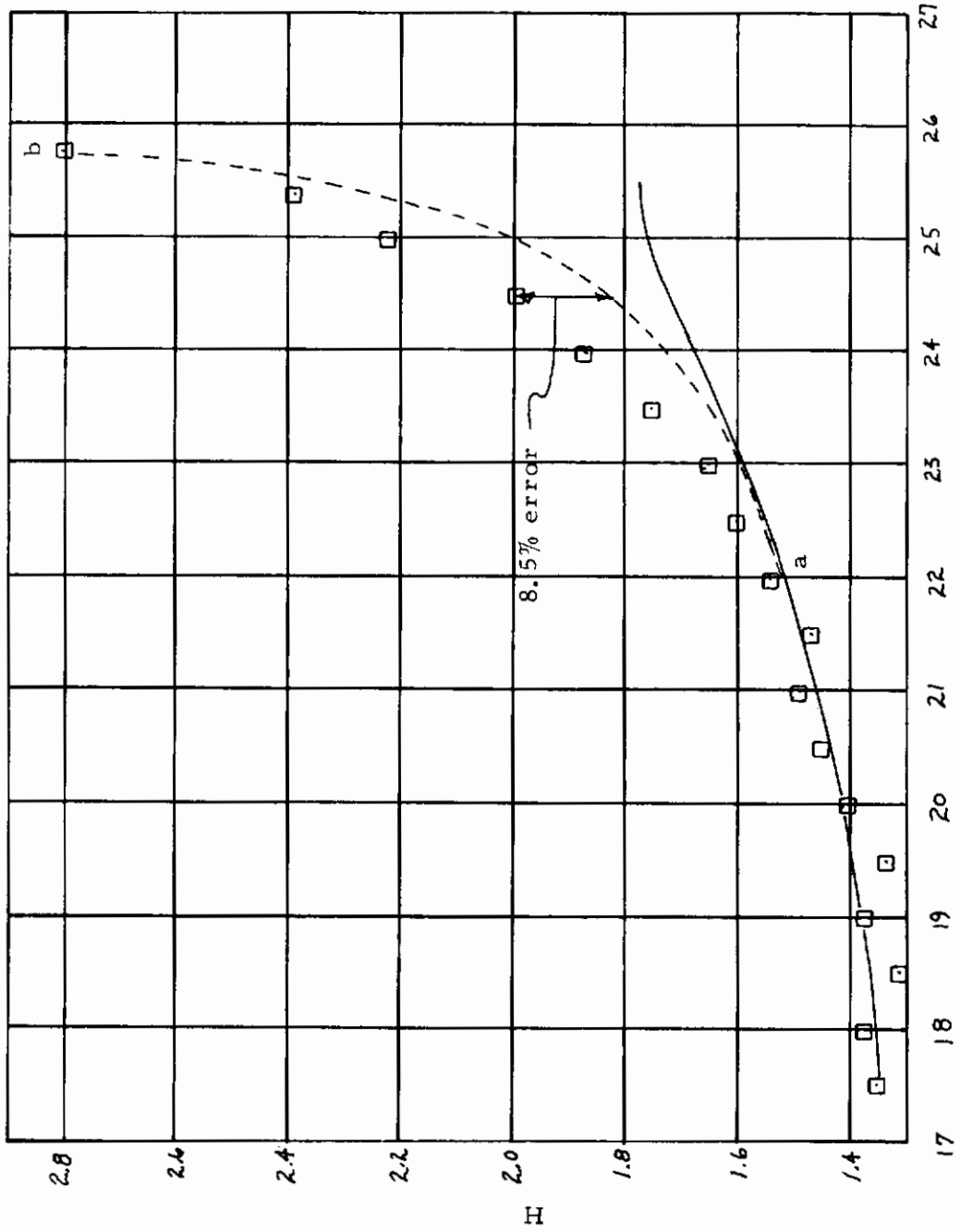

Figure 14. Comparisons of Calculations with the Data of Schubauer and Klebanoff.

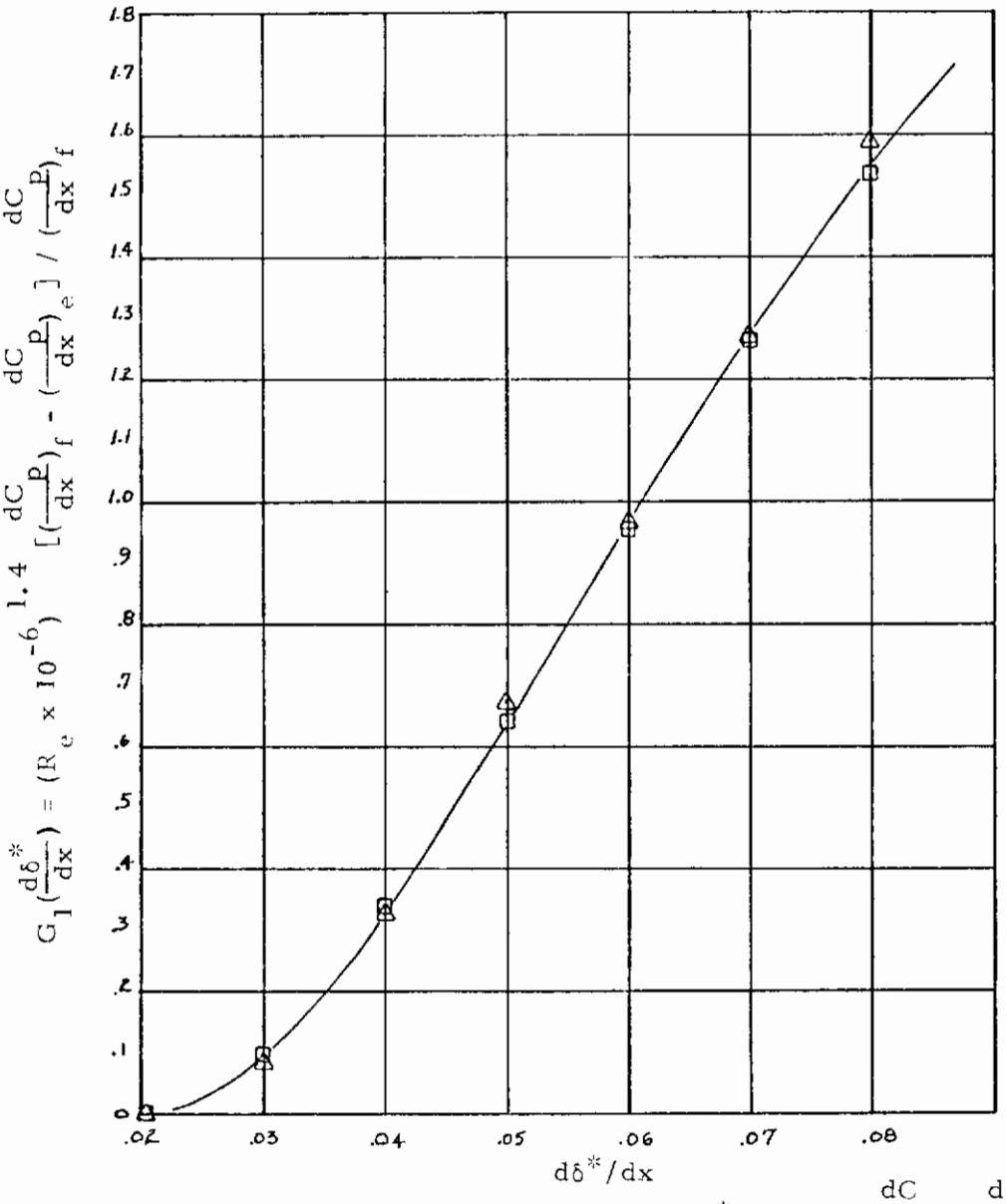

Figure 15. Empirical Correlation Between $d\delta^*/dx$ and $[(\frac{dC_p}{dx})_t - (\frac{dC_p}{dx})_e]$.

Unclassified
Security Classification

DOCUMENT CONTROL DATA - R&D
(Security classification of title, body of abstract and indexing annotation must be entered when the overall report is classified)

1. ORIGINATING ACTIVITY (Corporate author) University of Dayton Research Institute Dayton, Ohio 45409	2a. REPORT SECURITY CLASSIFICATION Unclassified 2b. GROUP N/A

3. REPORT TITLE
METHOD FOR THE PREDICTION OF PERFORMANCE OF STOL HIGH LIFT SYSTEMS NEAR $C_{L_{max}}$

4. DESCRIPTIVE NOTES (Type of report and inclusive dates)
Final Report (Jan 71 - Sept 71)

5. AUTHOR(S) (Last name, first name, initial)
BAUER, PAUL T.

6. REPORT DATE December 1971	7a. TOTAL NO. OF PAGES 52	7b. NO. OF REFS 24

8a. CONTRACT OR GRANT NO. AF33615-70-C-1019 b. PROJECT NO. 1366 c. Task Area Number: 17 d. Work Unit Number: 020	9a. ORIGINATOR'S REPORT NUMBER(S) AFFDL-TR-71-169 9b. OTHER REPORT NO(S) (Any other numbers that may be assigned this report) (None)

10. AVAILABILITY/LIMITATION NOTICES
Approved for public release; distribution unlimited

11. SUPPLEMENTARY NOTES	12. SPONSORING MILITARY ACTIVITY Air Force Flight Dynamics Laboratory Wright-Patterson Air Force Base, Ohio

13. ABSTRACT

Potential flow and boundary layer methods are identified and developed for the analytic calculation of the performance of lift systems with significant flow separation. Particular emphasis is given to the use of the presented methods in the calculation of the flow field for a single airfoil in demonstration of their capability. A procedure for application to multiple element high lift systems is indicated. Special consideration is given to the representation of turbulent separating boundary layers and an empirical computational procedure has been developed where none had previously existed. The work presented herein provides a thorough basis on which to develop an accurate computer simulation model of high lift systems with significant flow separation.

DD FORM 1 JAN 64 1473

UNCLASSIFIED
Security Classification

UNCLASSIFIED

Security Classification

14. KEY WORDS	LINK A		LINK B		LINK C	
	ROLE	WT	ROLE	WT	ROLE	WT
High Lift System Flow Separation Potential Flow Methods Boundary Layer Methods						

INSTRUCTIONS

1. ORIGINATING ACTIVITY: Enter the name and address of the contractor, subcontractor, grantee, Department of Defense activity or other organization *(corporate author)* issuing the report.

2a. REPORT SECURITY CLASSIFICATION: Enter the overall security classification of the report. Indicate whether "Restricted Data" is included. Marking is to be in accordance with appropriate security regulations.

2b. GROUP: Automatic downgrading is specified in DoD Directive 5200.10 and Armed Forces Industrial Manual. Enter the group number. Also, when applicable, show that optional markings have been used for Group 3 and Group 4 as authorized.

3. REPORT TITLE: Enter the complete report title in all capital letters. Titles in all cases should be unclassified. If a meaningful title cannot be selected without classification, show title classification in all capitals in parenthesis immediately following the title.

4. DESCRIPTIVE NOTES: If appropriate, enter the type of report, e.g., interim, progress, summary, annual, or final. Give the inclusive dates when a specific reporting period is covered.

5. AUTHOR(S): Enter the name(s) of author(s) as shown on or in the report. Enter last name, first name, middle initial. If military, show rank and branch of service. The name of the principal author is an absolute minimum requirement.

6. REPORT DATE: Enter the date of the report as day, month, year; or month, year. If more than one date appears on the report, use date of publication.

7a. TOTAL NUMBER OF PAGES: The total page count should follow normal pagination procedures, i.e., enter the number of pages containing information.

7b. NUMBER OF REFERENCES: Enter the total number of references cited in the report.

8a. CONTRACT OR GRANT NUMBER: If appropriate, enter the applicable number of the contract or grant under which the report was written.

8b, 8c, & 8d. PROJECT NUMBER: Enter the appropriate military department identification, such as project number, subproject number, system numbers, task number, etc.

9a. ORIGINATOR'S REPORT NUMBER(S): Enter the official report number by which the document will be identified and controlled by the originating activity. This number must be unique to this report.

9b. OTHER REPORT NUMBER(S): If the report has been assigned any other report numbers *(either by the originator or by the sponsor)*, also enter this number(s).

10. AVAILABILITY/LIMITATION NOTICES: Enter any limitations on further dissemination of the report, other than those imposed by security classification, using standard statements such as:

(1) "Qualified requesters may obtain copies of this report from DDC."

(2) "Foreign announcement and dissemination of this report by DDC is not authorized."

(3) "U. S. Government agencies may obtain copies of this report directly from DDC. Other qualified DDC users shall request through _____."

(4) "U. S. military agencies may obtain copies of this report directly from DDC. Other qualified users shall request through _____."

(5) "All distribution of this report is controlled. Qualified DDC users shall request through _____."

If the report has been furnished to the Office of Technical Services, Department of Commerce, for sale to the public, indicate this fact and enter the price, if known.

11. SUPPLEMENTARY NOTES: Use for additional explanatory notes.

12. SPONSORING MILITARY ACTIVITY: Enter the name of the departmental project office or laboratory sponsoring *(paying for)* the research and development. Include address.

13. ABSTRACT: Enter an abstract giving a brief and factual summary of the document indicative of the report, even though it may also appear elsewhere in the body of the technical report. If additional space is required, a continuation sheet shall be attached.

It is highly desirable that the abstract of classified reports be unclassified. Each paragraph of the abstract shall end with an indication of the military security classification of the information in the paragraph, represented as *(TS)*, *(S)*, *(C)*, or *(U)*.

There is no limitation on the length of the abstract. However, the suggested length is from 150 to 225 words.

14. KEY WORDS: Key words are technically meaningful terms or short phrases that characterize a report and may be used as index entries for cataloging the report. Key words must be selected so that no security classification is required. Identifiers, such as equipment model designation, trade name, military project code name, geographic location, may be used as key words but will be followed by an indication of technical context. The assignment of links, rules, and weights is optional.

GPO 886-551

☆U.S.Government Printing Office: 1972 — 759-082/370

UNCLASSIFIED

Security Classification